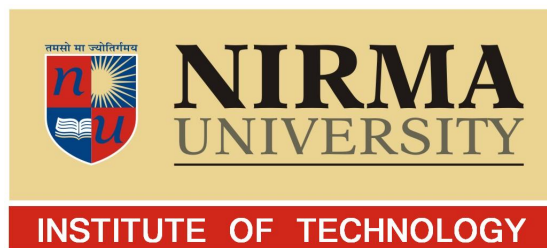


# DEVELOPMENT AND ANALYSIS OF CARBON FIBER SHAFT

By

Mitesh N. Zinzuvadia

11MMED16



DEPARTMENT OF MECHANICAL ENGINEERING

INSTITUTE OF TECHNOLOGY

NIRMA UNIVERSITY

AHMEDABAD-382481

MAY-2013

# DEVELOPMENT AND ANALYSIS OF CARBON FIBER SHAFT

Major Project

*Submitted in Partial Fulfillment of the Requirements for the degree of*

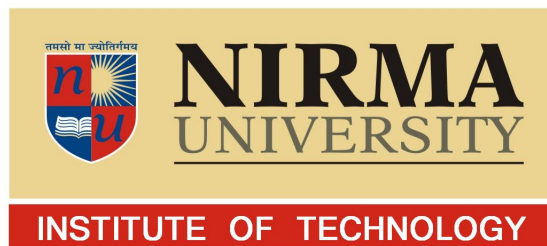
Master of Technology in Mechanical Engineering

(Design Engineering)

By

Mitesh N. Zinzuvadia

11MMED16



DEPARTMENT OF MECHANICAL ENGINEERING

INSTITUTE OF TECHNOLOGY

NIRMA UNIVERSITY

AHMEDABAD-382481

MAY-2013

# Declaration

This is to certify that

- i) The thesis comprises my original work towards the degree of Master of Technology in Mechanical Engineering at Nirma University and has not been submitted elsewhere for a degree.
- ii) Due acknowledgement has been made in the text to all other material used.

Mitesh N. Zinzuvadia

## Undertaking for Originality of the Work

I, **Mitesh N .Zinzuvadia**, Roll.No.**11MMED16**, give undertaking that the Major Project entitled “**Development and Analysis of Carbon-fiber shaft**” submitted by me, towards the partial fulfillment of the requirements for the degree of Master of Technology in Mechanical Engineering (Design Engineering) of Nirma University, Ahmedabad, is the original work carried out by me and I give assurance that no attempt of plagiarism has been made. I understand that in the event of any similarity found subsequently with any published work or any dissertation work elsewhere; it will result in severe disciplinary action.

\_\_\_\_\_  
Signature of Student

**Date:** \_\_\_\_\_

**Place:** NU, Ahmedabad

**Endorsed By**

**(Signature of Guide)**

# Certificate

This is to certify that the Major Project Report entitled **DEVELOPMENT AND ANALYSIS OF CARBON FIBER SHAFT** submitted by **Mr. Mitesh N. Zinzuvadia (Roll No: 11MMED16)** towards the partial fulfillment of the requirements for Degree of Master of Technology (Mechanical Engineering) in the field of Design Engineering from Nirma University is the record of work carried out by him under our supervision and guidance. The work submitted has in our opinion reached a level required for being accepted for examination. The results embodied in this major project work to the best of our knowledge have not been submitted to any other University or Institution for award of any degree or diploma.

## **Project Guide**

Prof. J. M. Dave

Department of Mechanical Engineering

Institute of Technology

Nirma University

Ahmedabad

## **Industry Guide**

Dr. B. K. Patel

Head of Department

Research and Development

Kemrock Industries and Exports Ltd.

Vadodara

## **Head of Department**

Department of Mechanical Engineering

Institute of Technology

Nirma University

Ahmedabad

## **Director**

Institute of Technology

Nirma University

Ahmedabad

## Acknowledgment

This is the product of research that was carried out at the Nirma University, Ahmedabad and Kemrock industries and Exports Limited (KIEL), Vadodara. I find great pleasure in expressing my gratitude to the people who have contributed to this work. I would like to start by thanking my project guide Prof. Jatinkumar M. Dave (Mechanical Engineering department, Institute of Technology, Nirma University) offering me the opportunity to join a very interesting research project and for believing in me always. I will never forget how much I have learned from the many interesting conversations we had about Mechanics of Composite Materials.

I am sincerely grateful to my industry guide Dr. B. K. Patel (Head of Department, RD, KIEL) for all the useful comments, discussions and the occasional laboratory testing.

I am indebted to Mr. Piyush Gupta (Head of departments, Pipes department, KIEL) and Mr. Sachin Patel (Head of department, Pultrusion department, KIEL). Who have trusted me and given opportunity to take this work. Also, I greatly appreciate the kindness and huge efforts of these two persons Mr. Chetan Patel (Former Manager, Pipes department. KIEL) and Mr. Shrikant Korde (Manager, Pultrusion department. KIEL) Our conversations were very enlightening for me.

I would like to thank Dr. D. S. Sharma (Head of mechanical engineering department, Institute of Technology, Nirma University), Dr. K. Kotecha (Director, Institute of Technology, Nirma University) and Management of Nirma University for allowing me to carry out my project at Kemrock Industries and Exports Limited, Vadodara. I express my sincere thanks to all faculties Members of collage who helped me during my M.Tech curriculum.

I am thankful to Mr. Shailesh Hemant (Head, Tooling department. KIEL) and Mr. Paresh Meruliya (Senior Design Engineer, KIEL) for the many times I went to both of them with a questions. My thanks go to all the other members of KIEL for their great help and friendship. Its been great working and having fun with my colleague Denish Kashipara, with whom Ive had the privilege of sharing knowledge.

I am greatly indebted to Mr. Umeshbhai Patel and Mr. Chetanbhai Soni who have provided me accommodation facilities during period of this research work. I am grateful to my Family. The loving support of my parents has been beyond words. I am blessed to have them in my life.

Most of all I am thankful to greatest God Swaminarayan and their follower H.H. Dhyani Swami by whose blessing I have successfully completed this work and I would like to dedicate this project to them.

**Mitesh N Zinzuvadia**

# Abstract

Due to High strength to weight ratio of carbon fiber composite provides higher natural frequency and can provide excellent performance instead of conventional steel shaft. This project mainly deals with the development and analysis of carbon fiber shaft for cooling tower coupling made by available resources at Kemrock Industries and Exports Limited, Vadodara. The company having 2-axis filament winding process and pull winding process machinery to manufacture shaft.

In this work, semi-empirical micromechanics approach based on Halpin-Tsai model is used to predict strength data for manufactured shaft. Comparison of theoretical and practical data is done to validate the results.

The output of this method is final shaft design and rovings arrangement required to manufacture an optimum shaft. The product is developed with pull-winding process. To validate analytical results, FEA cum laminate solver Hypersizer is used here. Also FEA results with ansys solver is shown here. Finally adhesive joint for flange design is discussed here.



## Abbreviation Notation and Nomenclature

FPF	.....	First ply failure
CLT	.....	Classical laminate theory
FEA	.....	Finite element Analysis
JAITEC	.....	Kemrock's commercial grade fibers
$E_{fL}$	.....	Longitudinal elastic modulus of fibers
$E_{fT}$	.....	Transverse elastic modulus of fibers
$E_m$	.....	Elastic modulus of matrix
$E_1$	.....	Longitudinal elastic modulus of lamina
$E_2$	.....	Transverse elastic modulus of lamina
$E_x$	.....	Laminate modulus in x-direction
$E_y$	.....	Laminate modulus in y-direction
$\nu_{fT}$	.....	Transverse poisson ratio of fiber
$\nu_m$	.....	Poisson's ratio of matrix
$\nu_{12}$	.....	Transverse poisson's ratio of lamina
$\nu_{xy}$	.....	Transverse poisson's ratio of laminate
$\nu_{yx}$	.....	Longitudinal poisson's ratio of laminate
$G_{fT}$	.....	Transverse shear modulus of fibers
$G_m$	.....	Shear modulus of matrix
$G_{12}$	.....	Transverse shear modulus of lamina
$V_f$	.....	Volume fraction for fiber
$V_m$	.....	Volume fraction for matrix
$\rho_f$	.....	Density of fibers
$\rho_m$	.....	Density of matrix
$\rho_c$	.....	Density of composite lamina
$(\sigma_f^A)_{ult}$	.....	Axial ultimate strength of fibers
$\sigma_{ft}$	.....	Tensile strength of fibers
$(\sigma_1^T)_{ult}$	.....	Transverse ultimate strength of lamina

$\sigma_{fc}$	.....	Compressive strength of composite
$\tau_f$	.....	Shear strength of fibers
$\tau_m$	.....	Shear strength of matrix
$\tau_{xy}$	.....	Shear strength of laminate
$(\epsilon_f)_{ult}$	.....	Ultimate strain of fibers
$T$	.....	Torque transmitted
$N_{xy}$	.....	Shear force
$r_m$	.....	Mean radius of shaft
$t$	.....	Laminate thickness
$W_f$	.....	Weight fraction of fibers
$W_m$	.....	Weight fraction of matrix
$m$	.....	Mass of shaft per meter length
$G_c$	.....	Shear modulus of adhesive
$e_c$	.....	Thickness of adhesive
$L$	.....	Length of shaft
$l$	.....	Length of adhesive bond

# Contents

<b>Declaration</b>	<b>iii</b>
<b>Undertaking</b>	<b>iv</b>
<b>Certificate</b>	<b>v</b>
<b>Acknowledgement</b>	<b>vi</b>
<b>Abstract</b>	<b>viii</b>
<b>Abbreviation Notation and Nomenclature</b>	<b>ix</b>
<b>List of Figures</b>	<b>xiv</b>
<b>List of Tables</b>	<b>xv</b>
<b>1 Introduction</b>	<b>1</b>
1.1 Benefits of Carbon fiber shaft . . . . .	1
1.2 Aim and Motivation . . . . .	2
1.3 Methodology . . . . .	6
1.3.1 Assumptions . . . . .	7
1.3.2 Load constraints . . . . .	7
1.3.3 Design Variable . . . . .	8
1.3.4 Design Constraints . . . . .	8
1.3.5 Design Method . . . . .	8
1.4 Outline of report . . . . .	10
<b>2 Literature review</b>	<b>11</b>
<b>3 Manufacturing of shaft with filament Winding process</b>	<b>14</b>
3.1 Introduction to process . . . . .	14
3.2 Process Description . . . . .	14
3.3 Winding pattern . . . . .	16
3.4 Trial Manufacturing . . . . .	18
3.5 Micromechanical Analysis of Helical-wounded shaft . . . . .	19

3.5.1	Analysis of $[\pm 30_2/90_5]$ Laminate shaft . . . . .	19
3.5.2	Failure criterion for a laminate . . . . .	21
3.6	Control Elements in Filament Winding . . . . .	23
3.6.1	Winding Angle . . . . .	23
3.6.2	Tension Control . . . . .	26
3.7	Result and Discussion . . . . .	27
<b>4</b>	<b>Development of shaft with Pull-Winding process</b>	<b>29</b>
4.1	Introduction to process . . . . .	29
4.2	Material Selection . . . . .	31
4.3	Micromechanical Analysis of pull-wounded shaft . . . . .	32
4.3.1	Trial manufacturing with $50 \times 2.5$ mm die . . . . .	32
4.4	Micromechanical analysis based on Halpin-Tsai Semi-empirical model	34
4.5	Theoretical calculation for Failure . . . . .	35
4.5.1	Torque transmission capacity . . . . .	35
4.5.2	Torsional buckling capacity . . . . .	35
4.5.3	Latural natural frequency . . . . .	35
4.6	Results and discussion . . . . .	35
4.7	Development of $60.33 \times 4.165$ Shaft . . . . .	36
<b>5</b>	<b>Testing of Composite specimens</b>	<b>38</b>
5.1	Tension Test in Accordance with ASTM D638 . . . . .	38
5.1.1	Specimen Preparation . . . . .	39
5.1.2	Test procedure . . . . .	39
5.2	Density Test in Accordance with ASTM D792 . . . . .	40
5.2.1	Test Procedure . . . . .	41
5.3	Fiber Volume Fraction in Accordance with ASTM D2584 . . . . .	42
5.3.1	Test Procedure . . . . .	43
<b>6</b>	<b>FEA and laminate analysis</b>	<b>45</b>
6.1	Introduction to Hypersizer . . . . .	45
6.1.1	Coupling to FEA . . . . .	45
6.1.2	Supported solvers . . . . .	46
6.2	Finite element analysis by Ansys . . . . .	46
6.3	Results and discussion . . . . .	47
6.3.1	Hypersizer Results . . . . .	48
6.3.2	Ansys results . . . . .	50
6.3.3	Comparison . . . . .	59
<b>7</b>	<b>Optimum Design</b>	<b>61</b>
7.1	New Layup arrangement . . . . .	61
7.2	Comparison between theoretical results and hypersizer results . . . . .	62
7.3	Finite Element analysis . . . . .	64
7.4	Results and discussion . . . . .	67

<b>8</b>	<b>Design of adhesive joints in composite drive shafts</b>	<b>68</b>
8.1	Adhesive joints . . . . .	68
8.2	Calculation for length and thickness of joint . . . . .	68
<b>9</b>	<b>Conclusion and Future work</b>	<b>71</b>
9.1	Concluding Remarks . . . . .	71
9.2	Future scope . . . . .	72
	<b>References</b>	<b>73</b>

# List of Figures

1.1	Installation of shaft . . . . .	3
1.2	Attachment of shaft . . . . .	3
1.3	Specifications of shaft . . . . .	3
1.4	All measurement specifications of shaft . . . . .	4
3.1	All axis configuration of filament winding machine . . . . .	16
3.2	Polar Winding . . . . .	17
3.3	Helical Winding . . . . .	17
3.4	Hoop Winding . . . . .	18
3.5	Schematic of fiber path in winding process . . . . .	24
4.1	Pull winding machine . . . . .	30
4.2	Co-axial winding on pultruded shaft . . . . .	30
5.1	D638 Specimen Configuration . . . . .	40
5.2	Axial Tensile Test set up . . . . .	41
5.3	D792 Specimen Configuration . . . . .	41
6.1	SHELL99 Linear layered structural shell . . . . .	47
6.2	Hypersizer result window . . . . .	48
6.3	Stress plot . . . . .	48
6.4	Hypersizer window for allowable load . . . . .	49
6.5	Ply failure window of Hypersizer . . . . .	49
6.6	XY shear stress - Nodal solution for 72mm shaft . . . . .	50
6.7	XY shear stress - Element solution for 72mm shaft . . . . .	51
6.8	First mode of lateral natural frequency for 72mm shaft . . . . .	52
6.9	XY shear stress - Nodal solution for 50mm shaft . . . . .	53
6.10	XY shear stress - Element solution for 50mm shaft . . . . .	54
6.11	First mode of lateral natural frequency for 50mm shaft . . . . .	55
6.12	XY shear stress - Nodal solution for 60.33mm shaft . . . . .	56
6.13	XY shear stress - Element solution for 60.33mm shaft . . . . .	57
6.14	First mode of lateral natural frequency for 60.33mm shaft . . . . .	58
6.15	XY shear for 60.33mm shaft . . . . .	59
6.16	XY shear comparison - analytical and ansys . . . . .	60
6.17	Lateral natural frequency comparison - analytical and ansys . . . . .	60

7.1	Standard Carbon fiber mats . . . . .	62
7.2	Hypersizer predicted properties for optimum design . . . . .	63
7.3	XY shear nodal solution . . . . .	64
7.4	XY shear element solution . . . . .	65
7.5	Modal analysis . . . . .	66
8.1	shear stress in cylindrical sleeve . . . . .	69
8.2	$\tau_{max}$ vs $\sqrt{e_c}$ graph for adhesive epoxy . . . . .	70

# List of Tables

1.1	Benefits of CF shaft . . . . .	1
1.2	Measurement specifications of shaft . . . . .	5
1.3	Bill of Materials . . . . .	5
3.1	Properties of AS4 Carbon Fiber . . . . .	19
3.2	Properties of Epoxy . . . . .	19
3.3	Thickness of each layer . . . . .	20
3.4	Predication of different parameters for AS4/Epoxy shaft . . . . .	23
3.5	Test result for 72 mm shaft . . . . .	28
4.1	Properties of 'JAITEC' Carbon Fiber . . . . .	32
4.2	Properties of Vinyl Ester KVR-6811 . . . . .	32
4.3	Trial shaft winding patterns . . . . .	33
4.4	Thickness of each layer for $50 \times 2.5$ shaft . . . . .	33
4.5	Test result for 50 mm shaft . . . . .	34
4.6	Predication of different parameters for 50 mm Pull wound shaft shaft . . . . .	34
4.7	No. of rovings required . . . . .	36
4.8	Roving sequence for $60.33 \times 4.165$ shaft . . . . .	36
4.9	Thickness of each layer for $60.33 \times 4.165$ shaft . . . . .	37
4.10	Predication of different parameters for 60.33 mm Pull wound shaft . . . . .	37
6.1	Comparison of theoretical, Hypersizer and practical result . . . . .	59
7.1	Layer configuration for optimum shaft . . . . .	61
7.2	Predication of different Lamina properties for JAITEC/Vinylester shaft . . . . .	62
7.3	Predication of different Laminate properties for JAITEC/Vinylester shaft . . . . .	63



# Chapter 1

## Introduction

### 1.1 Benefits of Carbon fiber shaft

With recent advance research and development in composite material due to Carbon Fiber Driveshaft have significantly higher torsional strength and less weight over popular aluminum or steel shafts and all other carbon composite driveshaft. Advantages of Carbon Fiber Driveshaft are Increased Vibration Dampening, Light Weight, Higher Natural Frequency, Patent-Pending Design, Higher RPM Capability, Engineered for Safety, Less Rotating Weight, Greatest Strength. Refer following table to get idea about its benefit.

Table 1.1: Benefits of CF shaft

<b>Features</b>	<b>Functions</b>	<b>Benefits</b>
Low weight	Reduced mass, Reduced bearing loads, Reduced Inertia	Simplified Installation, Increase bearing life, Reduce vibration
Corrosion Resistance	Resist Chemical attack	Extend service life, Reduced maintenance, Increase safety
Low co-efficient of Thermal Expansion	Dimensional stability	Reduced Vibration, Reduced stress, Increase operating range

Continuous fiber composite spacer flange	Infinite flange life	Low cost of ownership
Utilized flex element	Eliminate Fretting, Infinite fatigue life, Simplified Installation	Low cost of ownership, Longer service life, Reduced maintenance, Increased safety
High misalignment capacity	Reduced equipment stress, Increase life	Easier Installation, Reduced ownership costs
High strength to weight ratio	Increase stiffness, Higher critical speed	Eliminate Harmonica, Eliminate steady bearings

Applications: Wind Speed Shaft; Car; Yacht Industries, Cooling Towers, and many more.

## 1.2 Aim and Motivation

Main reason of having throughout performance of composite cooling towers is benefits of carbon fiber shaft discussed in previous section. Rexnord Industries[1], LLC, pioneered and introduced the first advanced composite couplings to the cooling tower industry in 1987. Also different methods of laminate analysis are all time favorite field of engineers. Kemrock Industries and Exports Limited is leading industry in India for all kind of Composite solution.

Industry is designing for Carbon fiber cooling tower coupling. Design parameters are fixed by customer. Here all parameters are discussed.

Following figures are showing installation and attachment of shaft in cooling tower. Input source is motor BHP and output source is fan BHP.

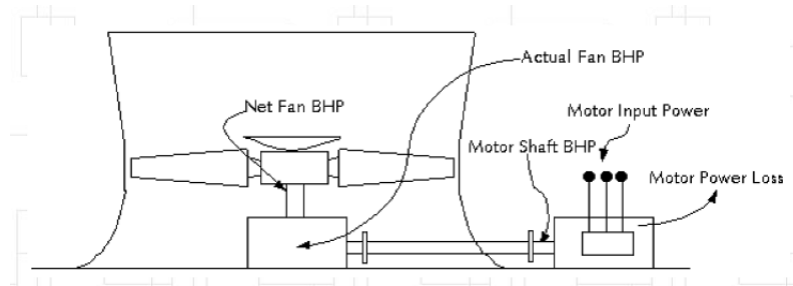


Figure 1.1: Installation of shaft

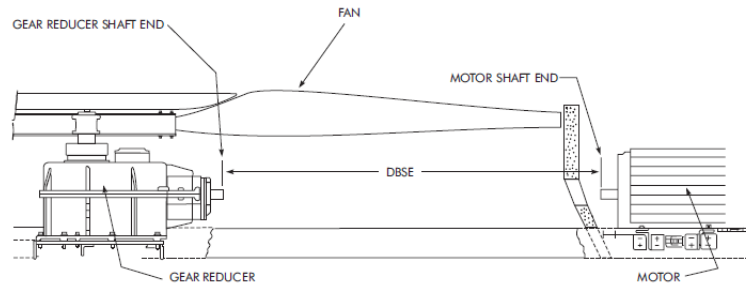


Figure 1.2: Attachment of shaft

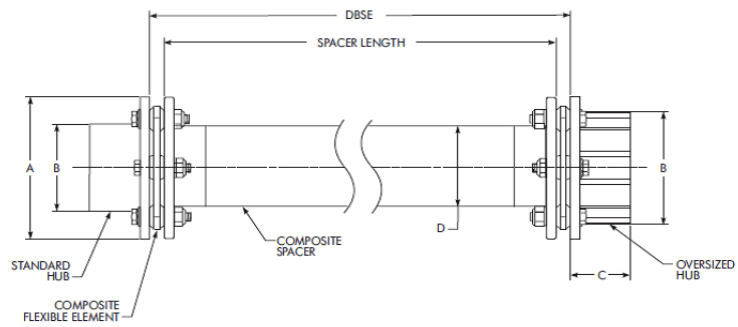


Figure 1.3: Specifications of shaft

Industry is going to produce composite coupling shaft for different range of cooling towers figure of different dimensions is shown here.[1].

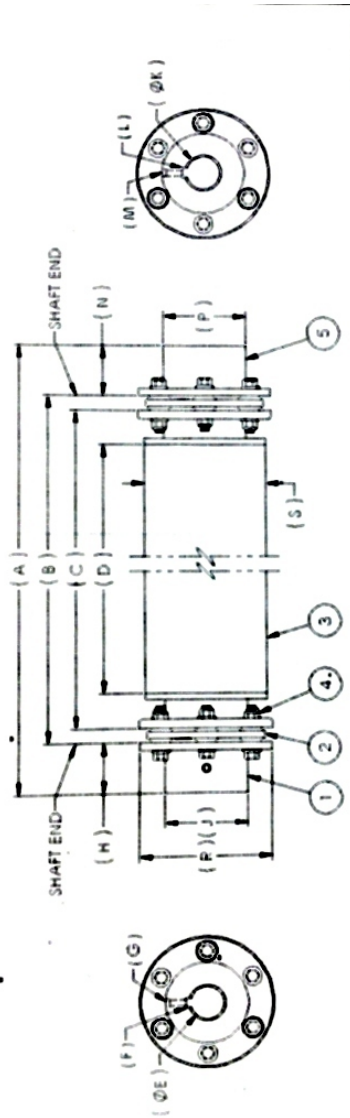


Figure 1.4: All measurement specifications of shaft

Table 1.2: Measurement specifications of shaft

<b>Sr.no</b>	<b>Measurement specifications</b>
A	Overall Length
B	DBSE
C	Spacer Length
D	Tube Length
E	Motor hub Bore
F	Motor hub Key
G	Motor hub set screw
H	Motor hub Length
J	Motor hub body OD
K	Gear hub bore
L	Gear hub key
M	Gear hub set screw
N	Gear hub Length
P	Gear hub body OD
R	Flange OD
S	Tube OD

Table 1.3: Bill of Materials

<b>Description</b>	<b>Material</b>	<b>Quantity</b>
Motor Hub	316 Stainless steel	1
Flex element	Composite	2
Spacer	Composite assembly	1
Hardware kit	316 Stainless steel	2
Gear Hub	316 Stainless steel	1

Performance specifications required by customer is listed below ofcourse considerable tolerences are applicable. Our design industry has to produce only tube and flange designs.

- Rated continuous torque @ 2.0 Safety factor = 621 Nm
- Peak overload torque = 1864 Nm
- Tube Length = 2000 mm
- shaft OD = 60.33 mm
- Flange OD = 152.4 mm
- Flange thickness = 16 mm
- Maximum weight of tube per meter = 1.4 Kg/m
- Frequency at critical speed = 46 Hz

To met with given customer specification trial shafts are made with available mandrel and dies.

### **1.3 Methodology**

Many methods are available at present for the design optimization of structural systems and these methods based on mathematical programming techniques. In the present work an attempt is made to evaluate the suitability of composite material such as Carbon/Epoxy and Carbon/Vinylester for the purpose of power applications. A one tube length of composite drive shaft for cooling tower coupling is to be made subjected to the constraints such as torque transmission, torsional buckling strength capabilities[14, 6] and here for given specifications the objective is to find no. of rovings and its winding pattern required to satisfy constraints.

### 1.3.1 Assumptions

The shaft rotates at a constant speed about its longitudinal axis. The shaft has a uniform, circular cross section. The shaft is perfectly balanced, i.e., at every cross section, the mass center coincides with the geometric center. All damping and nonlinear effects are excluded. The stress-strain relationship for composite material is linear and elastic; hence, generalized Hooks law is applicable for composite materials.[2] Since lamina is thin and no out-of-plane loads are applied, it is considered as under the plane stress.

### 1.3.2 Load constraints

The shaft is considered as simply supported beam undergoing transverse vibration or can be idealized as a pinned-pinned beam.[9] Natural frequency can be found using following theory.

Bernoilli-Euler beam theory neglects both transverse shear deformation as well as rotary inertia effects.[15] Natural frequency based on this theory is given by following equation.

$$f_x = \frac{\pi}{2} \sqrt{\frac{E_x I}{m L^4}} \quad (1.1)$$

Shear strength is main criterion for torque transmission and given by,

$$\tau = \frac{16 T d_0}{\pi (d_0^4 - d_i^4)} \quad (1.2)$$

Since long thin hollow shafts are vulnerable to torsional buckling[14], the possibility of the torsional buckling of the composite shaft was checked by the expression for the torsional buckling load of a thin walled orthotropic tube and which is expressed below.

$$T_c = (2\pi r_m^2 t)(0.272)(E_x E_y^3)^{\frac{1}{4}} \left(\frac{t}{r_m}\right)^{\frac{3}{2}} \quad (1.3)$$

### 1.3.3 Design Variable

No of rovings i.e. fiber volume fractions, tube thickness, fiber orientation angles are design variable

### 1.3.4 Design Constraints

Lateral natural frequency as per equation 1.1 is depended on axial modulus so  $E_x$  and  $m$  are design constraint. Other design constraints are Torque transmitted =  $T \leq T_{max}$  and Torsional buckling capacity =  $T_c \geq T_{max}$

### 1.3.5 Design Method

In all standards books like [3] classical laminate theory is described which is applicable to plain lamina Here small portion of shaft is considered as flat laminate. Also micromechanics approach [19] is used to define Lamina properties.

The stress in kth ply are[8]

$$\begin{pmatrix} \sigma_x \\ \sigma_y \\ \tau_{xy} \end{pmatrix} = \begin{pmatrix} \bar{Q}_{11} & \bar{Q}_{12} & \bar{Q}_{16} \\ \bar{Q}_{21} & \bar{Q}_{22} & \bar{Q}_{26} \\ \bar{Q}_{16} & \bar{Q}_{26} & \bar{Q}_{66} \end{pmatrix} \begin{pmatrix} \epsilon_x^0 \\ \epsilon_y^0 \\ \gamma_{xy}^0 \end{pmatrix} \quad (1.4)$$

Knowing the stresses in each ply, the failure of the laminate is determined using the First Ply Failure criteria. That is, the laminate is assumed to fail when the first ply fails. Here maximum stress theory is used to find the torque transmitting capacity.

Different relations based on micromechanics approach of Semi-empirical model of Halpin-Tsai [3] are used.

$$E_1 = E_f V_f + E_m V_m \quad (1.5)$$



$$\frac{E_2}{E_m} = \frac{1 + \xi\eta V_f}{1 - \eta V_f} \quad (1.6)$$

$$\eta = \frac{\frac{E_{fT}}{E_m} - 1}{\frac{E_{fT}}{E_m} + \xi} \quad (1.7)$$

$$\frac{G_{12}}{G_m} = \frac{1 + \xi\eta V_f}{1 - \eta V_f} \quad (1.8)$$

$$\eta = \frac{\frac{G_{fT}}{G_m} - 1}{\frac{G_{fT}}{G_m} + \xi} \quad (1.9)$$

$$\nu_{12} = \nu_{fT} V_f + \nu_m V_m \quad (1.10)$$

$$\rho_c = \rho_f V_f + \rho_m V_m \quad (1.11)$$

$$(\sigma_1^T)_{ult} = (\sigma_f^A)_{ult} V_f + (\epsilon_f)_{ult} E_m (1 - V_f) \quad (1.12)$$

$$\tau_{12} = (\tau_f) V_f + (\tau_m) V_m \quad (1.13)$$

Here  $\xi$  is reinforcing factor and depends on micro geometry here assume that fibers are circular and arrange in square array.

## 1.4 Outline of report

In next chapter literature survey for given problem is described then in chapter 3 trial from 2-axis filament winding machine is discussed. Also it is discussed that axial properties can't be achieved by this process due to fiber orientation angle limitation and then next chapter 4 in which laminate analysis based on Halpin-Tsai model and classical laminate theory is done for pull wound shaft in which we can see torque transmission capacity is not achieved without  $\pm 45$  degree mat.

Chapter 5 describes different test standards used by Kemrock industry and other standards for different mechanical testing. Chapter 6 mainly deals with FEA analysis, also laminate analysis by Hypersizer solver is shown there. Comparison of theoretical result and other results are shown there.

Chapter 7 describes optimised stacking sequence for given specifications This shaft and its results are discussed in this chapter. Also FEA and theoretical analysis shows this shaft is safe and satisfy all design constraints. And after obtaining optimum design the adhesive bonding for flanges are discussed in chapter 8. Finally conclusion is written in last chapter.

# Chapter 2

## Literature review

One of the most useful book for all is Mechanics of Material by Kaw [8] from which we got aware about basic mechanics of composite materials. No doubt other books such as Tsai, Vasiliev, Daniel [19] [18] [3] from which it was understood the behavior of composite material under application of different loads. Ply, Layers and laminate behavior extensively defined by [18]

From this study it was understood that classical laminate theory can be applied here for our problem and then first ply failure criteria can be used for such a plain stress problem.

In our case where final laminaproperties are not available, the military handbooks [12] [11] becomes helpful to us fo predication of fiber and matrix properties. Halphin and Tsai [19] [13] developed their models as simple equations by curve fitting to results that are based on elasticity. The equations are semi-empirical in nature because involved parameters in the curve fitting carry physical meaning.

Almost all engineering material possesses to a certain extent the property of elasticity. If the external forces producing deformation do not exceed a certain limit, the deformation disappears with the removal of the forces so it is assumed by [16] that the bodies undergoing the action of external forces are perfectly elastic. With this assumption equations are used.

Most of the methods used for design optimization assume that the design variables are continuous. [15, 17, 14] In structural optimization, almost all design variables are discrete. A simple Genetic Algorithm (GA) is used to obtain the optimal number of layers, thickness of ply and fiber orientation of each layer. All the design variables are discrete in nature and easily handled by GA. With reference to the middle plane, symmetrical fiber orientations are adopted.

Durability issues [7] to be considered in each case include the potentially degrading effects that both cyclic and sustained loadings, exposure to automotive fluids, temperature extremes, and low-energy impacts from such things as tool drops and kickups of roadway debris can have on structural strength, stiffness, and dimensional stability. The basic in-air properties provided for the reference composite, while interim in nature, are intended to serve as a baseline for planning the remaining durability tests for the composite. Two fiber orientations are addressed:  $0^{\circ}/90^{\circ}$  relative to the specimen axis and  $+45^{\circ}$ . These orientations result in two extremes of behavior. In the tensile loading case, the behavior of specimens with the  $0/90^{\circ}$  fiber orientation is fiberdominated, while for specimens with the  $45^{\circ}$  fiber orientation, the behavior is very much matrix dominated. [13]

Designing a filament winding machine involves two major components. [5] First com-

ponent is the designing of the mechanism which delivers appropriate winding pattern as specified by the user (i.e. the winding angle). The second component is the realization of an effective fiber tensioning system for ensuring consistent overall consolidation.

Cooling tower fundamentals [6] provides deep knowledge of elements used in cooling tower. Also it shows Blade pass natural frequency affects the shaft frequency. For this reason in our research permissible frequency is taken 46 Hz instead of 30 Hz at motor speed of 1800 RPM.

Composite design and application by Tsai[9] has specified different criteria for failure of adhesive bond. Also Kim[17] has done detailed analysis on composite adhesive bond.

# Chapter 3

## Manufacturing of shaft with filament Winding process

### 3.1 Introduction to process

Filament Winding is one of the most widely used processes for manufacturing axis-symmetric objects. Despite all its limitation the easier and most accurate way of producing axis-symmetric parts, is filament winding. Moreover, since it can be highly automated; it is quite economical in mass production. The applications of filament winding range are very wide; it includes pressure vessels, chemical tanks, aircraft fuselages, rocket motor cases, helicopter rotor shafts, high pressure pipelines, sporting goods, wind turbine blades and other structural applications. This chapter deals with the composite manufacturing process of filament winding and outlines the key control aspects in a filament winding process.

### 3.2 Process Description

Filament winding is a process, where fibers after being wetted in a resin, are positioned on rotating mandrel under controlled tension, by a carrier following on a specific pattern which establishes winding angle. The winding angle is achieved by

controlling the carrier velocity with respect to the mandrel rotation. The winding angle is the angle between fibers and mandrel axis of rotation. In a winding process, the angles can vary from perpendicular to the longitudinal axis of the mandrel to any angle other than being parallel to the axis. The layers which are perpendicular to the axis are called hoop layers and the layers at an angle to the axis are called the helical layers.

According to Hazra[5], the filament winding process is a reverse mechanism of a lathe operation. The way a lathe removes material from the rotating mandrel at a required rate and quantity, the filament winding machine adds material to a rotating mandrel. As the mandrel rotates, the carriage travels along the mandrel length and delivers fiber on the mandrel with a controlled position and tension. Mandrel rotation, the carriage velocity and carriage position are controlled by the winder controller and these parameters define the winding pattern.

Filament winding machines are categorized by their degrees of freedom. The minimum degrees of freedom possible are two, first the rotation of mandrel and second the horizontal movement of the carriage. For a two axis winder the delivery eye can be integral part of the horizontal carrier. Other possible degrees of freedom can be additional movement of the delivery eye, like vertical movement, rotational movement and forward and backward motions. To date, the maximum number of axis available on a filament winder are seven. Figure below shows all probable degrees of freedom that are possible in filament winding machine. The degrees of freedom, other than the two obvious two degrees of freedom, are indicated by red arrows and the later part of the Figure shows all the seven possible degrees of freedom.

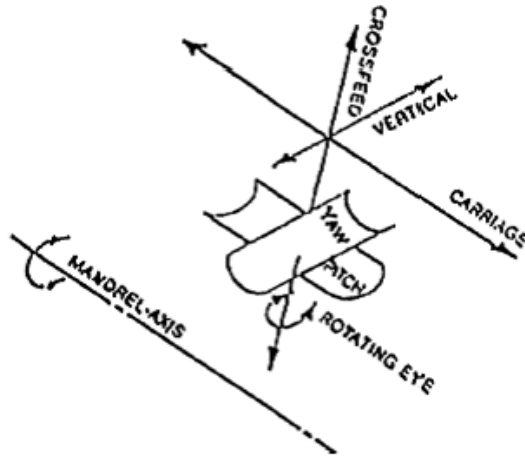
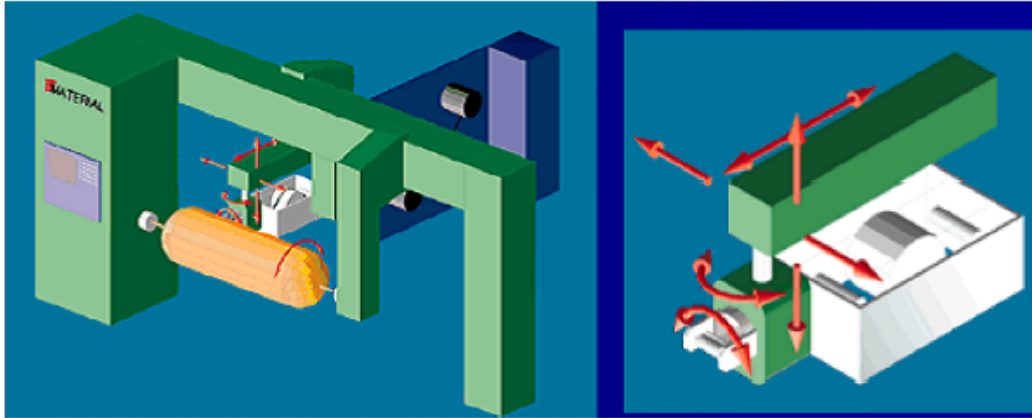


Figure 3.1: All axis configuration of filament winding machine

### 3.3 Winding pattern

Filament-wound products are produced by using one of the three basic types of winding patterns: polar, helical, and hoop. The choices made are based on the shape of the part and the reinforcement orientations required. Polar winding is used to lay down fiber close to  $0^\circ$  to the longitudinal axis. Polar windings generally pass close to or around the mandrel poles. Each completed polar winding pattern covers the mandrel surface with a single layer of reinforcements Fig. 3.2. Helical winding is used to lay fiber at angles from  $5^\circ$  to  $80^\circ$  to the longitudinal axis. These fibers are wound on the mandrel surface in alternating positive and negative orientations and



result in a double layer of wound material. Helical windings may pass around the end of a closed-end shape Fig. 3.3. Hoop winding is a special form of helical winding and is used to deposit fiber close to  $90^\circ$  to the longitudinal axis. Hoop windings are generally applied only to the cylindrical or straight portion of a mandrel and result in a single layer of reinforcement material Fig. 3.4

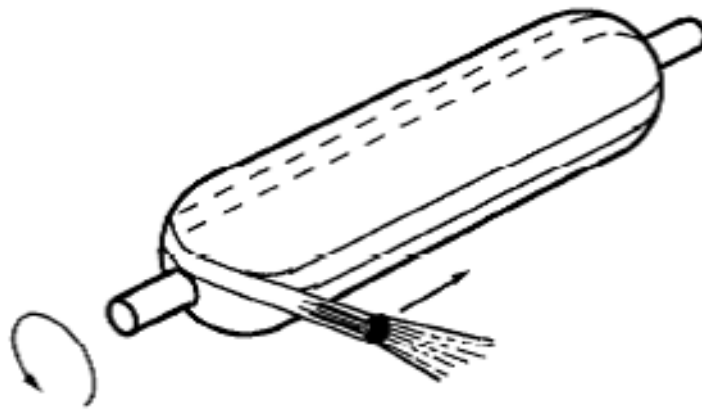


Figure 3.2: Polar Winding

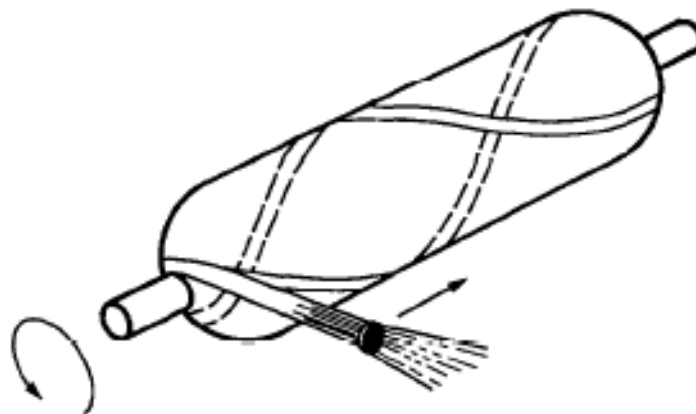


Figure 3.3: Helical Winding

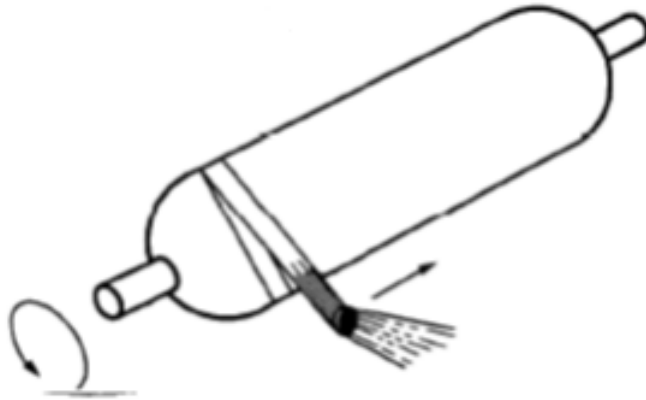


Figure 3.4: Hoop Winding

But unfortunately in Kemrock only two-axis conventional winding machine is available in which twisting of fibers cant be avoided which plays major role in lowering laminate strength also minimum angle can be wound with this machine is  $30^{\circ}$ .

### 3.4 Trial Manufacturing

In begiing few trial manufacturing were done in which Latural natural frequency of shaft was found lower than required. Here trial of shaft is made with standard AS4 commercial grade carbon fiber and Epoxy resin is shown. Epoxy resin is known for its incredible toughness and bonding strength. Quality epoxy resins stick to other materials with 2,000-p.s.i. vs. only 500-p.s.i. for vinyl ester resins and even less for polyesters.

In areas that must be able to flex and strain with the fibers without micro-fracturing, epoxy resins offer much greater capability. Cured epoxy tends to be very resistant to moisture absorption. Epoxy resin will bond dissimilar or already-cured materials which make repair work that is very reliable and strong. Epoxy actually bonds to all sorts of fibers very well and also offers excellent results in repair-ability when it

is used to bond two different materials together. Initially, epoxy resin is much more difficult to work with and requires additional skill by the technicians who handle it.

Table 3.1: Properties of AS4 Carbon Fiber

Parameter	Values
$E_{fL}$	235 GPa
$E_{fT}$	15 GPa
$G_{12}$	27 GPa
$\nu_{fT}$	0.20
$\rho_f$	1810 $Kg/m^3$
$\sigma_{ft}$	3700 MPa
$\sigma_{fc}$	1999 MPa
$\tau_f$	36 MPa

Table 3.2: Properties of Epoxy

Parameter	Values
$E_m$	3.4 GPa
$G_{12}$	1.26 GPa
$\nu_m$	0.36
$\rho_m$	1170 $Kg/m^3$
$\sigma_{mt}$	80 MPa
$\sigma_{mc}$	104 MPa
$\tau_m$	40 MPa

## 3.5 Micromechanical Analysis of Helical-wounded shaft

### 3.5.1 Analysis of $[\pm 30_2/90_5]$ Laminate shaft

To achieve high strength, winding configured as  $[\pm 30_2/90_5]$  where layer thicknesses are decided by following measurement

Mandrill OD = 63.7 mm

OD of shaft after two  $\pm 30$  circuits and 3 hoops = 70.4 mm

OD of shaft after 5 hoops = 72 mm

If we assume all hoops have covered equal thickness and all  $30^0$  windings covered equal thickness than in laminate than arithmetically thickness of each layer are as below.

Table 3.3: Thickness of each layer

Layer no.	Angle	Thickness in mm
1	90	0.4
2	-90	0.4
3	90	0.4
4	-90	0.4
5	90	0.4
6	-30	0.5375
7	30	0.5375
8	-30	0.5375
9	30	0.5375

So analysis is based on Halpin-Tsai semi-empirical formulas as below where Hydrothermal effects are not considered

$W_f$  and  $W_m$  as per ASTM 2584 [4] testing are 52% and 48% respectively

In terms of the fiber and matrix volume fractions. In terms of individual constituent properties, the mass fractions and volume fractions are related by

$$W_f = \frac{\frac{\rho_f}{\rho_m} V_f}{\frac{\rho_f}{\rho_m} V_f + V_m} \quad (3.1)$$

$$W_m = \frac{V_f}{\frac{\rho_f}{\rho_m} (1 - V_m) + V_m} \quad (3.2)$$

So from above equations  $V_f$  and  $V_m$  found 41.2% and 58.8% respectively.

### 3.5.2 Failure criterion for a laminate

A laminate will fail under increasing mechanical and thermal loads. The laminate failure, however, may not be catastrophic[11]. It is possible that some layer fails first and that the composite continues to take more loads until all the plies fail. Failed plies may still contribute to the stiffness and strength of the laminate. The degradation of the stiffness and strength properties of each failed lamina depends on the philosophy followed by the user.

- When a ply fails, it may have cracks parallel to the fibers. This ply is still capable of taking load parallel to the fibers. Here, the cracked stiffness, transverse tensile strength, and shear strength. The longitudinal modulus and strength remain unchanged.
- When a ply fails, fully discount the ply and replace the ply of near zero stiffness and strength. Near zero values avoid singularities in stiffness and compliance matrices.

The procedure for finding the successive loads between first ply failure and last ply failure is described below.

- a. Given the mechanical loads, apply loads in the same ratio as the applied loads. However, apply the actual temperature change and moisture content.
- b. Use laminate analysis to find the mid-plane strains and curvatures.
- c. Find the local stresses and strains in each ply under the assumed load.
- d. Use the ply-by-ply stresses and strains in ply failure theories discussed in [8, 3, 19], to find the strength ratio. Multiplying the strength ratio to the applied load gives the load level of the failure of the first ply. This load is called the first ply failure load.

- e. Degrade fully the stiffness of damaged ply or plies. Apply the actual load level of previous failure.
- f. Go to step b to find the strength ratio in the undamaged plies:
  - If the strength ratio is more than one, multiply the strength ratio to the applied load to give the load level of the next ply failure and go to step b.
  - If the strength ratio is less than one, degrade the stiffness and strength properties of all the damaged plies and go to step e.
- g. Repeat the preceding steps until all the plies in the laminate have failed. The load at which all the plies in the laminate have failed is called the last ply failure.

In our case for carbon-epoxy laminate predicted lamina properties for 0.412% fiber volume fraction as per Tsai-Wu failure criterion is calculated. Here Hydrothermal effects are not considered also some parameters which are affected in process is not considered. By finding strength from above procedure it shows difference between theoretical and practical result as below.

Theoretically for first ply failure as per Tsai-Wu failure criterion is  $\sigma_{xt} \approx 85.02 \text{ MPa}$  Where practical value for  $\sigma_{xt}$  found as 147 MPa  $\downarrow$  85.02 which shows theoretical value of strength is nearer to practical one But there are some other parameters which effects the performance of shaft.

Now Halpin-Tsai equations 1.5 to 1.13 are used to predict lamina properties. Here it was assumed that[3] fibers are circular and arranged in square array of Geometry than predication of final lamina and laminate properties are as under.

Table 3.4: Predication of different parameters for AS4/Epoxy shaft

Parameter	Values
$E_1$	98.82 GPa
$E_2$	6.264 GPa
$G_{12}$	2.774 GPa
$\nu_{12}$	0.294
$\rho_c$	1433.68 $Kg/m^3$
$(\sigma_1^T)_{ult}$	1556 MPa
$E_x$	15.74GPa
$E_y$	20.70 GPa
$G_{xy}$	6.552
$\nu_{xy}$	0.241
$\nu_{yx}$	0.318
$(\sigma^T)_{ult}$	85.02 MPa
$\tau_{xy}$	35.84

## 3.6 Control Elements in Filament Winding

The major control parameters in a filament winding as discussed above are winding angle and winding tension, which contribute primarily to the strength of the produced composites.

### 3.6.1 Winding Angle

As discussed above the winding machine in general consists of at least two major moving parts; first, the rotating system on which the mandrel rotates, and second, the fiber delivery system or the carrier which is linear in motion. The composite manufacturing as discussed earlier is produced by layers of reinforcement bonding together by a resin matrix. The formation of every layer in a composite manufacturing process is critical. Orientation of the fibers in each layer contributes to the characteristics and strength of the composite. In filament winding the orientation of the fiber layout is governed by the winding angle of the machine. Hazra [5] analyzed the effect of winding angle on the tensile strengths of the composite. They summarized that with the increase in winding angle, the circumferential tensile strength increases and

the axial strength decreases.

When the fiber is wound and completes one full cycle through entire length of a mandrel, then one circuit is formed. In practice, due to continuous and complete motion, the fiber may not reach the starting point after its complete cycle. In fact, due to an offset reach of a different point it might take more than one cycle of the entire length for the fiber to reach the start point; when the winding reaches that point, it is referred to as pattern. Finally, a layer is the number of patterns required to cover the entire mandrel surface with fiber. The mathematical calculations below formulate the winding angle and then demonstrate how the winding angle is related to circuit, pattern and finally to the layer.

Considering a helical winding pattern; Figure below shows the path followed by the fiber in a winding operation. Let  $\alpha$  = Winding angle in radians

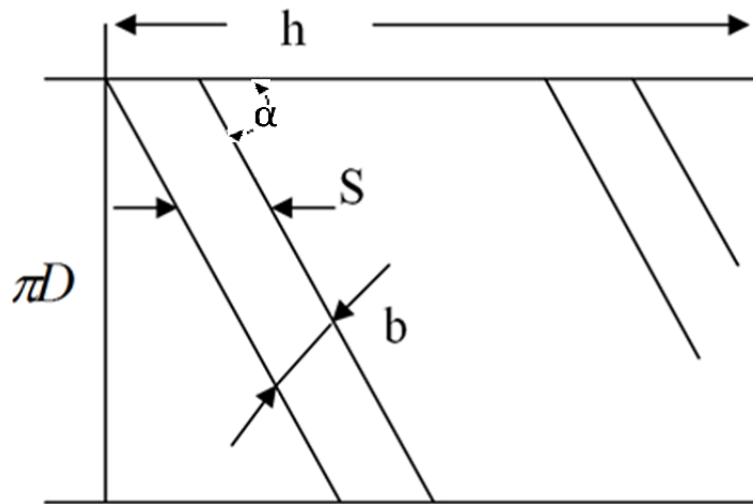


Figure 3.5: Schematic of fiber path in winding process



We get:

$$\tan\alpha = \frac{N_m\pi D}{60v_c}$$

Where,  $v_c$  = Carrier velocity (m/s)

$N_m$  = Mandrel Velocity (RPM)

$D$  = Diameter of mandrel (m)

The length covered by a single bandwidth of fiber in one mandrel revolution can be established by:

$$\frac{\pi D}{\tan\alpha}$$

If  $h$ , is the total mandrel length, then the number of revolutions required to cover the whole mandrel can be established by.

$$n = \frac{h}{L} = \frac{h \tan\alpha}{\pi D} = \frac{h N_m}{60 V_c}$$

If  $S$  is the circumferential coverage with fiber of bandwidth,  $b$  and winding angle, then

$S$ , can represented by

$$S = \frac{b}{\cos\alpha}$$

So number of circuits per layer, C can be calculated as:

$$C = \frac{\pi D}{S} = \frac{\pi D 60 v_c}{b \sqrt{(60 v)^2 + (\pi D N_m)^2}}$$

### 3.6.2 Tension Control

The tension in the fiber is one of the major factors which accounts for 70% of products stiffness and tensile strength [10]. Fiber tension contributes for volume fraction, which is a measure of the compactness of the fiber and is dependent on the winding tension.[10] This confirms the relationship of the fiber stress and the tolerance of the internal pressure by the composite. Also, it can be seen that the longitudinal and horizontal stresses are a function of the winding angle . The relationship is explained mathematically below.

The stress in fiber,  $\sigma_f$ , in a fiber can be broken into components stress (i.e. longitudinal and circumferential stresses respectively) [10].

$$\sigma_y = \frac{pr}{2t} \text{ and } \sigma_x = \frac{pr}{t} \text{ where}$$

p is Internal Pressure ( $N/m^2$ )

r is Radius of Cylinder (m)

t is Thickness (m)

A is Fiber-band Cross Section Area, which includes resin. ( $m^2$ )

$\sigma_x; \sigma_y$  = Longitudinal and Hoop Stress Respectively ( $N/m^2$ )

$\sigma_f$  = Resultant fiber stress in the direction of the winding angle ( $N/m^2$ )

Summing up the stress components in equations

$$\sigma_f = \frac{\sqrt{5}pr}{2t}$$

Equation shows how the internal pressure tolerance can be controlled by the stress of fiber. If T, is the instantaneous fiber tension then;

$$\sigma_f = \frac{T}{AV_f}$$

where  $V_f$  is the fiber volume fraction.

Equation shows that tension in the fiber contributes to fiber stress [10]. Also adding of adequate tension in the fiber eliminates voids in the winding increasing the tension, decreasing the viscosity and winding speed can reduce the void content to 1%. [7] The presence of a void air gap reduces , the stress handling capacity of the fiber, considerably. This makes the tension control a very important parameter of the filament winding process. In other words, the pressure handling capability of a wound composite is governed by the number of layers, the winding angle and fiber tension.[5] Improper or inconsistent fiber tension disturbs the winding angle as well.

### 3.7 Result and Discussion

By applying failure criteria we can obtain Laminate strength for given orientation. Also some Laminate parameters are tested practically as per ASTM test standards[4]. Practical results are shown below. Our theoretical laminate axial strength obtained here as per first ply failure criterion is 85.02 MPa. Which shows theoretical and practical values are not differing much and our theory is reliable Other parameters are

Table 3.5: Test result for 72 mm shaft

Sr. No.	Parameter	Method	Value
1	Tensile Stength	ASTM D638	147 MPa
2	Carbon content by weight	ASTM D2584	52%

not tested practically but for caluation of frequency, torque capacity and torsional buckling capacity we will take theoretical predications from Halpin-Tsai equations.

**Shear stress indused in 72 mm shaft** For given peak torque of 1864 Nm we have to apply similar shear load in classical laminate theory. This is given by following equation;

$$N_{xy} = \frac{T}{2\pi r_m^2} \quad (3.3)$$

So here  $N_{xy} = 257766.41$  N/m and maximum shear stress induced in global cordinates are 138.3 MPa. Which is greater than safe shear stress of 35.84 MPa so design will fails in torsion.

#### **Lateral natural frequency**

Frequency found from equation 1.1 is 31.27 Hz which is lower than required so shaft will vibrates at its critical speed.

Result from Hypersizer software of laminate analysis which is discussed in chapter - 6 shows without polar winding we can't achieve axial modulus as high as required for permissible lateral natural frequency. Which is not possible on 2-axis polar winding machine. Hypersizer shows maximum modulus of Elasticity obtained for winding angle of  $30^0$  and  $45^0$  is approximately 20 GPa So newer 4-axis machine or process should be implemented. Company has already modified their one pultrusion machinary in pull winding machinary. Next chapter deals with the shafts made with pullwinding process.

# Chapter 4

## Development of shaft with Pull-Winding process

### 4.1 Introduction to process

Pullwinding is a method of producing high performance composite tubes combining the techniques of conventional pultrusion and continuous filament winding. Layers of axial fibers and helically wound fibers are combined to produce a product with an excellent crush strength, high stiffness and superb torsional properties. Pullwound profiles are available in glass or carbon fiber in combination with polyester, vinylester, or epoxy resin systems. The ratio of axial reinforcement to helical reinforcement can be varied to suit the specific requirements of the end use of the products. The technology enables to optimize the wall thickness, strength and stiffness while retaining the low weight.

Disadvantage of this process is only suitable for continuous production and single piece of shaft can be costly. Figures below are showing machine of pull-winding process and co-axial winding on pultruded shaft.

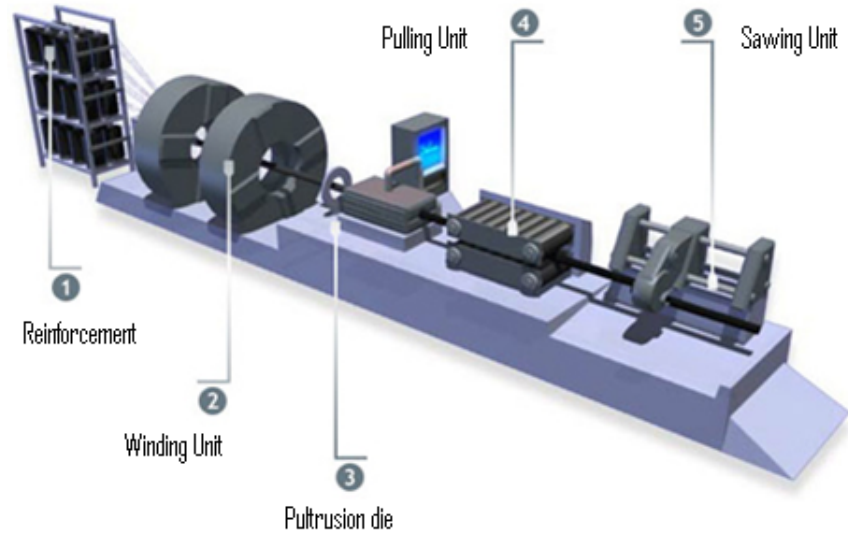


Figure 4.1: Pull winding machine

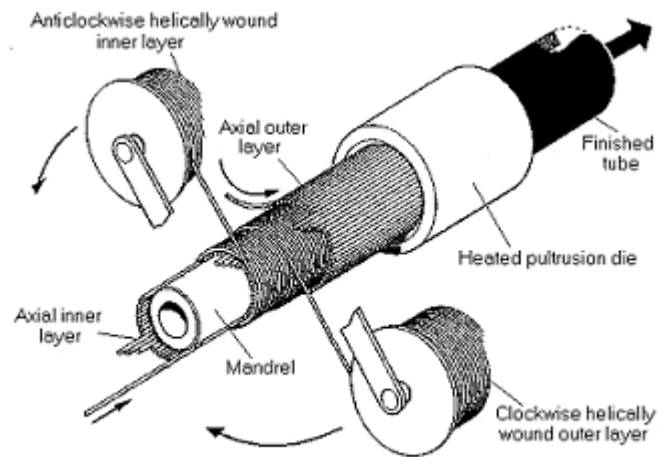


Figure 4.2: Co-axial winding on pultruded shaft

## 4.2 Material Selection

We already have Kemrocks JAITEC commercial grade carbon fiber and different resins but Vinylester resins are stronger than polyester resins and cheaper than epoxy resins. Vinylester resins utilize a polyester resin type of cross-linking molecules in the bonding process. Vinylester is a hybrid form of polyester resin which has been toughened with epoxy molecules within the main molecular structure. Vinylester resins offer better resistance to moisture absorption than polyester resins but its downside is in the use of liquid styrene to thin it out (not good to breath that stuff) and its sensitivity to atmospheric moisture and temperature. Sometimes it won't cure if the atmospheric conditions are not right. It also has difficulty in bonding dissimilar and already-cured materials. It is not unusual for repair patches on vinylester resin canoes to delaminate or peel off. As vinylester resin ages, it becomes a different resin (due to its continual curing as it ages) so new vinylester resin sometimes resists bonding to your older canoe, or will bond and then later peel off at a bad time.

It is also known that vinylester resins bond very well to fiberglass, but offer a poor bond to kevlar and carbon fibers due to the nature of those two more exotic fibers. Due to the touchy nature of vinylester resin, careful surface preparation is necessary if reasonable adhesion is desired for any repair work. But self lubrication property is developed in Kemrock's HVR-6811 Vinylester resin which will be responsible for low die damage and also it has lower cost so it is decided to take Kemrocks Vinylester KVR-6811 resin with JAITEC fibers for pull winding process. Also Kemrock has developed self lubrication property in Vinylester so better suitable for die.

Table 4.1: Properties of 'JAITEC' Carbon Fiber

Parameter	Values
$E_{fL}$	180 GPa
$E_{fT}$	14 GPa
$G_{12}$	19 GPa
$\nu_{fT}$	0.20
$\rho_f$	1760 $Kg/m^3$
$\sigma_{ft}$	2300 MPa
$\sigma_{fc}$	1990 MPa
$\tau_f$	29 MPa

Table 4.2: Properties of Vinyl Ester KVR-6811

Parameter	Values
$E_m$	3.4 GPa
$G_{12}$	1.1 GPa
$\nu_m$	0.32
$\rho_m$	1200 $Kg/m^3$
$\sigma_{mt}$	78.45 MPa
$\sigma_{mc}$	101 MPa
$\tau_m$	41 MPa

## 4.3 Micromechanical Analysis of pull-wounded shaft

### 4.3.1 Trial manufacturing with 50×2.5 mm die

First trial shaft is made with available 50×2.5 mm die. Roving patterns and thickness occupied by each rovings are calculated below. Theoretically calculated mass of shaft per meter

$$m = [\rho_f V_f + \rho_m V_m] A$$

Here from experimental data as per ASTM 2584 says  $W_f = 77.23\%$  and  $W_m = 22.77\%$

So  $V_f = 0.6981$  and  $V_m = 0.3019$



Table 4.3: Trial shaft winding patterns

Layer no.	No. of Rovings	Angle of winding
1	64	0
2	1	90
3	63	0
4	1	90
5	63	0

Predication of lamina thickness is based on formula as below.

$$t = \frac{A_w}{\rho_f V_f} \quad (4.1)$$

Where  $A_w$  is areal weight.

Here winding pattern are [0/90/0/90/0]

Now fiber roving weight is 1.5 g/m so for first layer  $A_w = 64 \times 1.5 \times 10^{-3} / 2 \times \pi \times 0.0025$

And Thickness = 0.497 mm. Similarly we can find thickness of each 0° roving and for 90° roving subtract it from laminate thickness. Finally we obtain following table.

Table 4.4: Thickness of each layer for 50 × 2.5 shaft

Layer no.	Angle	Thickness in mm
1	0	0.544
2	90	0.472
3	0	0.515
4	90	0.472
5	0	0.497

## 4.4 Micromechanical analysis based on Halpin-Tsai Semi-empirical model

Carbon fibers are transversely isotropic fibers so according to Halpin-Tsai theory[19, 3] best results obtained by relations given in the chapter 1. We have following test results. Now by using semi-empirical model of Halpin-Tsai predicted properties are

Table 4.5: Test result for 50 mm shaft

Sr. No.	Parameter	Method	Value
1	Tensile Stength	ASTM D638	548 MPa
2	Density	ASTM D792	1521.7 $Kg/m^3$
3	Carbon content by weight	ASTM D2584	77.23%
4	Resin contents (without considering voids)	ASTM D2584	22.77%

as under,

Table 4.6: Predication of different parameters for 50 mm Pull wound shaft shaft

Parameter	Values
$E_1$	126.7 GPa
$E_2$	9.13 GPa
$G_{12}$	4.715 GPa
$\nu_{12}$	0.2362
$\rho_c$	1590.94 $Kg/m^3$
$(\sigma_1^T)_{ult}$	1619 MPa
$E_x$	82.53 GPa
$E_y$	53.62 GPa
$G_{xy}$	4.715
$\nu_{xy}$	0.040
$\nu_{yx}$	0.026

## 4.5 Theoretical calculation for Failure

Our design is not as per OD given by customer but this is just for comparative study.

### 4.5.1 Torque transmission capacity

Here required torque capacity for shaft is 1864 Nm. Now according to equation[ ], for first ply failure criterion  $\tau_{12} = 35.69$  MPa. Therefore  $T = 301.24Nm$   
So according to FPF criterion this design is not safe in torsion.

### 4.5.2 Torsional buckling capacity

Torsional buckling capacity for this shaft is 6940.9 Nm which is very higher than peak overload torque 1864 Nm. So shaft will not buckle torsionally.

### 4.5.3 Latural natural frequency

According to Euler-Bernoli equation  $f_{neb} = 50.11$  Hz  $\geq$  46 Hz. So resonance will not occure at drive speed.

## 4.6 Results and discussion

This design of shaft is not as per customer requirement but this is done for evaluting the correct volume fraction of fibers because with 69.81% fiber volume fraction this product becomes rough finished and fibers can be seen from surface. Here experimen-tal trials by industry in filament winding and pultrusion products shows that 50% to 60% fiber volume fractions are required to high finished look.

Finally new die as per customer requirement is designed.

## 4.7 Development of $60.33 \times 4.165$ Shaft

Finally as per customer requirement we have made die for  $60.33 \times 4.165$  shaft. By using the previous study we can calculate for new die. For 50% to 60% fiber volume fraction Excel table is made as following.

Table 4.7: No. of rovings required

$V_f$	No. of rovings
0.4	269.46
0.45	308.77
0.5	349.57
0.55	391.94
0.6	435.98
0.65	481.79
0.7	529.47

So here for 50% to 55% weight fraction following roving arrangement selected for  $[0/90/0/90/0]$  ply sequence.

Table 4.8: Roving sequence for  $60.33 \times 4.165$  shaft

Layer no.	Angle	No. of rovings
1	0	144
2	90	1
3	0	108
4	90	1
5	0	108
<b>Total</b>		362

Lamina thickness are

By further using micromechanics approach and FPF criterion predicted properties for this shaft are as below.

Lateral natural frequency is higher for this shaft it will be 57.52 Hz but torque transmission capacity of this shaft is 624.38 Nm so this shaft will fail in torsion.

Table 4.9: Thickness of each layer for  $60.33 \times 4.165$  shaft

Layer no.	Angle	Thickness in mm
1	0	1.490
2	90	0.0625
3	0	1.254
4	90	0.0625
5	0	1.296

Table 4.10: Predication of different parameters for 60.33 mm Pull wound shaft

Parameter	Values
$E_1$	80.21 GPa
$E_2$	6.415 GPa
$G_{12}$	2.489 GPa
$\nu_{12}$	0.268
$\rho_c$	1443.38 Kg/m <sup>3</sup>
$(\sigma_1^T)_{ult}$	1025 MPa
$E_x$	78.10 GPa
$E_y$	8.637GPa
$G_{xy}$	2.489
$\nu_{xy}$	0.199
$\nu_{yx}$	0.022

Torsional buckling capacity for this shaft is 4798.36 Nm which is higher than torque transmission capacity so shaft will not buckle torsionally. Also we can say that there is no need of  $90^0$  rovings for next design but we should add  $45^0$  rovings for better torque capacity.

# Chapter 5

## Testing of Composite specimens

Kemrock industry has different test facilities for tensile strength, flexural strength, density and fiber content. Industry mainly prefers American Standards for Testing of Materials (ASTM). All ASTM standards are discussed well by [4] and [20]. Three main standards used in our research is discussed here.

### 5.1 Tension Test in Accordance with ASTM D638

The ASTM D638 standard test method was devised for determining the in-plane tensile properties of un-reinforced and reinforced plastics in the form of standard dumbbell-shaped test specimens (ASTM D638, 2002). The standard recommends the specimen configuration, the apparatuses needed to measure the specimen width and thickness, the testing fixture needed to conduct the test, and the desired strain measuring device. The following sections explain the specimen configuration, the specimen preparation and the different apparatuses used to conduct the test. Any deviation from the standard is noted and explained.

### 5.1.1 Specimen Preparation

Referring to the standard, at least 5 specimens should be tested per testing condition. To account for specimen data that may be lost during the testing process or data analysis, 8 specimens for each direction were tested. Each panel had two orthogonal directions: x-direction and y-direction, where the x-direction is the laminate principal axis. The specimens were cut from the panels with a water-abrasive jet. The dimensions of the specimens were in accordance with Type I shown in figure 5.1 of ASTM Standard D638. The dimensions were 165.1 mm (6.5 in) for the overall length, 19.05 mm (0.75 in) for the overall width, 57.15 mm (2.25 in) for the length of the narrow section, 12.7 mm (0.5 in) for the width of the narrow section, and 76.2 mm (3 in) for the radius of the fillet. The witness panels were manufactured with 8 layers of fabric resulting in a total thickness of approximately 5.08 mm (0.2 in), which met the recommended thickness in figure 1 of the standard (ASTM D638, 2002). Since the fabric used is woven with an aerial weight of  $817.13 \text{ g/m}^2$  (24.1 oz/yd<sup>2</sup>), the surface of the panel that was not on the mold was wavy with a thickness tolerance of approximately 14%. The thickness tolerance of the specimens did not meet the requirements of the standard which was  $\pm 4\%$  of the thickness. The specimen dimensions are shown in figure 5.1. The specimens were conditioned in accordance with procedure C of test method D5229 (ASTM D5229/D5229M, 2002)[4].

### 5.1.2 Test procedure

The specimen was gripped in the testing machine with a distance of 114.3 mm (4.5 in) between the grips and the grip heads were rotationally self-aligning. The testing machine was a servo controlled hydraulic machine with the capability of controlling the velocity of the moving head. The testing machine was capable of indicating the total load being carried by the test specimen with a maximum capacity of 100 kN. The specifications of the testing machine were in conformance with ASTM Practices E4 (ASTM E4, 2002). The test was conducted with a constant head speed of 1.2

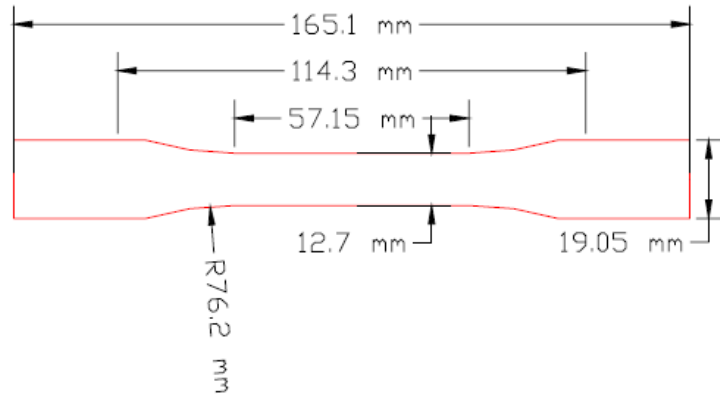


Figure 5.1: D638 Specimen Configuration

mm/min (0.047 in/min) and each test elapsed between approximately two and a half minutes and three minutes. The load and strain data were collected at a rate of approximately 1 hertz, or one data point every second. The strain data collected was a full-field strain of the area of interest of the specimen. Then strength can be calculated by basic equation of stress,  $\text{stress} = \text{Load}/\text{minimum area}$

## 5.2 Density Test in Accordance with ASTM D792

The density of the PMC with woven fabric reinforcement was measured in accordance with ASTM D792 standard test method. The standard contained two methods to follow depending on the material under study. Since the panels in this study are PMC, method A was chosen which was specified for testing solid plastics in water. The other method, method B, was for testing solid plastics in liquids other than water (ASTM D792, 2000).

Five specimens were cut out of each panel for density measurement. The specimen configuration was selected to meet the requirements of the apparatus used for con-





Figure 5.2: Axial Tensile Test set up

ducting the test. The specimens were cut to a size as large as the immersion vessel could hold. A large specimen was selected to increase the accuracy of the test and reduce the variability arising from errors while conducting the test. A 2d-CAD drawing of the specimen configuration is shown in Figure 5.3. The specimens were conditioned in accordance to procedure C of test method D5229 (ASTM D5229/D5229M, 2002).

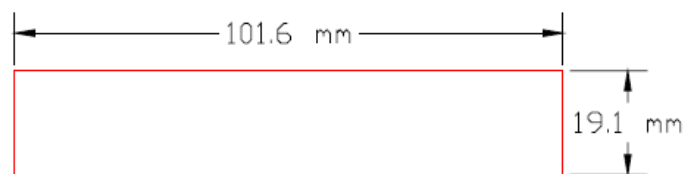


Figure 5.3: D792 Specimen Configuration

### 5.2.1 Test Procedure

The rooms temperature and relative humidity were recorded; similarly, the temperature of the distilled water was measured and recorded. The weight of each specimen

in air was measured and recorded using a digital balance with a precision of 0.1 mg ( $3.5 \times 10^{-6} \text{oz}$ ) according to the recommendation of the standard. A plastic beaker was used as the immersion vessel. It was partially filled with distilled water to a height of at least the specimen submersion depth. The weight of the filled beaker was zeroed out prior to starting. A rigid wire was used to carry the specimen in water; in order to correct for the buoyant force of the submergible portion of the wire, it was measured separately and recorded. The buoyant force was considered to be the weight of the item fully submerged in water. The latter was achieved by submerging the item into the beaker and reading the scale display. The buoyant force of the specimen with the metal wire was measured by holding the specimen with the metal wire and lowering both, the specimen and wire, into the water. The reading on the scale was recorded and used with the previous indicated reading to calculate the density of the specimen. The density of the specimen was calculated by the use of equation

$$D = w / \frac{a - b}{c}$$

where.

D = density of the specimen,  $g/cm^3$ ,

w = mass of specimen in air g,

a = mass of the specimen and portion of the metal wire completely immersed in water, g,

b = mass of the portion of the metal wire immersed in water, g,

c = density of the distilled water at the temperature measured,  $g/cm^3$

## 5.3 Fiber Volume Fraction in Accordance with ASTM

### D2584

The standard test method for ignition loss of cured reinforced resins, ASTM D2584, was designed for the determination of the resin content of a composite. Assuming

the void content of the PMC under study as negligible, the resin content was used to determine the fiber volume fraction of the composite using the densities of the fabric and resin.

The standard test method for ignition loss of cured reinforced resins, ASTM D2584, was designed for the determination of the resin content of a composite. Assuming the void content of the PMC under study as negligible, the resin content was used to determine the fiber volume fraction of the composite using the densities of the fabric and resin. The specimens were conditioned in accordance to procedure C of test method D5229 (ASTM D5229/D5229M, 2002).

### **5.3.1 Test Procedure**

The crucible weight was measured ( $W$ ) using a digital balance with a precision of 0.1 mg ( $3.5 \times 10^{-6}oz$ ) according to the recommendation of the standard. Each specimen was placed in a crucible and the combined mass of the crucible and the specimen were measured ( $W1$ ) using the same digital balance. The crucibles containing the specimens were then placed into an electric furnace and heated to a temperature of  $400^{\circ}C$  ( $752^{\circ}F$ ) for five to ten minutes. The specimens were then ignited using a butane torch. Once all the specimens had self-extinguished, the temperature of the furnace was increased to  $565^{\circ}C$  ( $1049^{\circ}F$ ) and the specimens were left for a period of five hours at that temperature. This process burned the resin and removed any carbonaceous material on the fabric of the composite. When the specimens were removed, the crucibles only contained clean layers of woven fabric that was reinforcing the PMC. When the specimens had cooled to room temperature the mass of the residue plus the crucible was measured ( $W2$ ). The weight fraction of the resin that was present in the specimen was obtained using equation.

$$W_R = \frac{W_1 - W_2}{W_1 - W}$$

where,

$W_R$  = weight fraction of the resin,

$W_1$  = weight of specimen and crucible, g (oz),

$W_2$  = weight of residue and crucible,

$W$  = weight of crucible, g (oz).

# Chapter 6

## FEA and laminate analysis

### 6.1 Introduction to Hypersizer

Hypersizer is FEA cum laminate solver which is developed by Collier research foundation and used by NASA for design of equipments for space application. Its outstanding capabilities are discussed here.

#### 6.1.1 Coupling to FEA

- Combine the capabilities of FEA and HyperSizer
- Develop an integrated capability where
- FEA provides
  - Global internal load paths
  - Global stiffness optimization
- HyperSizer provides
  - Detailed design strength and stability analyses
  - Local sizing optimization
- Supports some leading FEA solvers and FEM modelers

### 6.1.2 Supported solvers

- Currently Supported
  - MSC/NASTRAN solver – bulk data file
  - I-DEAS solver and modeler – universal file
  - FEMAP modeler– neutral file
  
- Planned to be Supported
  - PATRAN modeler
  - ANSYS solver and modeler

Also laminate solver of HyperSizer has all the functionality of composite laminate analysis) plus stress analysis and detailed design optimization using any material for 50 different stiffened and sandwich panels and open cross section beams. The user can apply general edge loadings and/or boundary conditions through the Free Body Diagram GUI and solve for the resulting stresses and structural integrity using over 100 different failure analyses. Analyses include traditional industry methods, modern analytical and computational solutions, and some unique approaches. Interaction between the engineer and the software is key to HyperSizer’s design process. Interactive graphics provide visual inspection of the structural concepts drawn-to-scale optimum panel and beam cross sections. These features are used to identify design flaws early. Built-in optimization provides lightweight designs automatically.

## 6.2 Finite element analysis by Ansys

In this research, finite element analysis is performed using ANSYS software. To model the composite shaft, the shell 99 element is used and the shaft is subjected to torsion. The shaft is fixed at one end in axial, radial and tangential directions and is subjected to torsion at the other end. After performing a static analysis of the shaft,

the maximum shear stress at midplanes of layers are equated with theoretical results. Also first Lateral natural frequency is counted with this solver which is equated with theoretical results.

Typical SHELL99 element configuration is shown below. This element allows user to choose upto 250 layers and according to [15] laminate is solved.

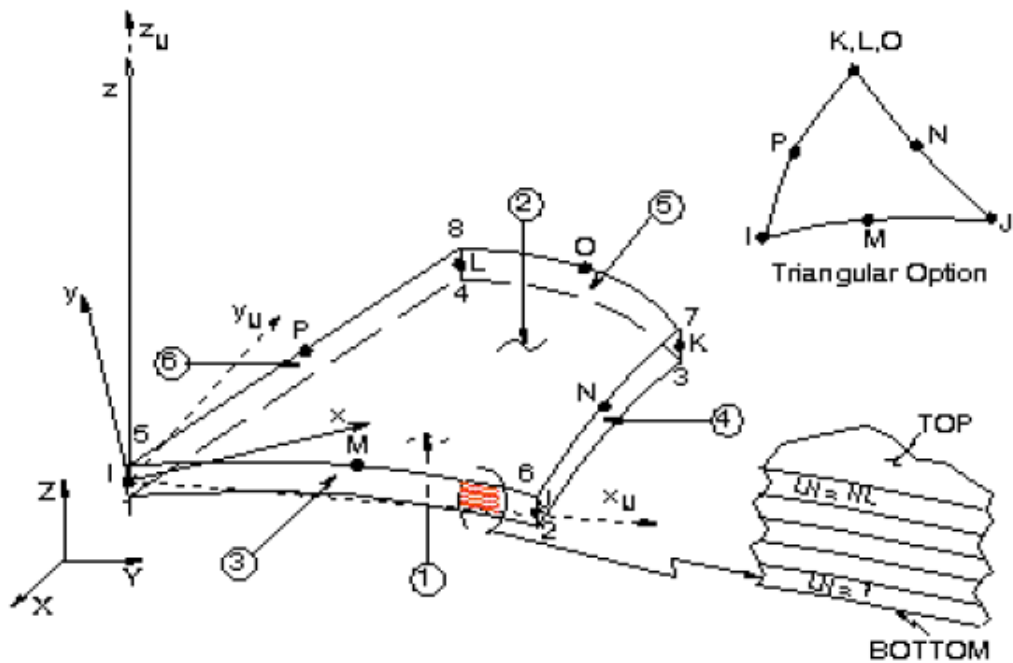


Figure 6.1: SHELL99 Linear layered structural shell

### 6.3 Results and discussion

In theoretical calculations, properties got by Halpin-Tsai equations are used to find Laminate strength both Hypersizer and Ansys results are as under.

Effective Laminate Elastic Engineering Constants										
E1	(Pa)	E2	(Pa)	$\nu_{12}$	G	(Pa)	Gxz	(Pa)	Gyz	(Pa)
1.574152E+10		2.069977E+10		0.2414778	6.551331E+09		2.773903E+09		2.773903E+09	

Effective Laminate Flexural Elastic Engineering Constants					Neutral Axis					
Ef1	(Pa)	Ef2	(Pa)	$\nu_{f12}$	Gf	(Pa)	X	(m)	Y	(m)
1.481864E+10		2.137585E+10		0.2178985	6.155759E+09		-8.127291E-04		8.273212E-04	

Effective Laminate Failure Allowables											
Fu1	(Pa)	Fu2	(Pa)	Fsu12	(Pa)	eu1	(m/m)	eu2	(m/m)	esu12	(m/m)
7.93503E+07		7.276987E+07		3.400095E+07		5.040829E-03		3.515491E-03		5.189931E-03	

Figure 6.2: Hypersizer result window

### 6.3.1 Hypersizer Results

Excellent Graphics capability of Hypersizer gives Different graphs. Stress plot is shown below.

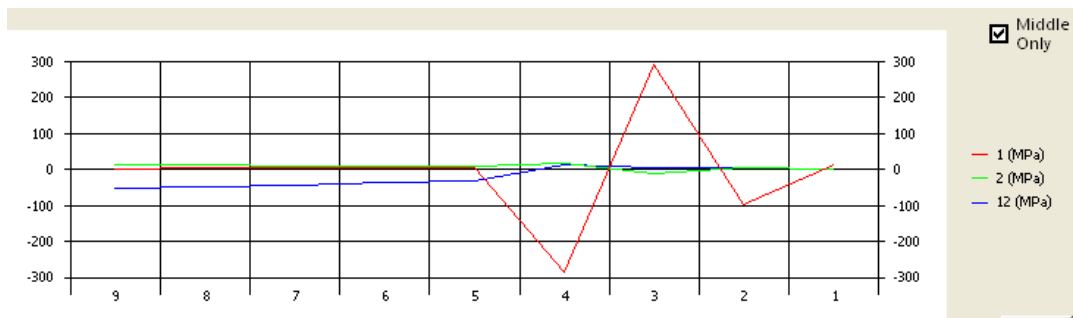


Figure 6.3: Stress plot

Also hypersizer can be useful to know ply failures and allowable load. For example on Gr/Ep laminate the shear load is applied.

From above window we can get ply failures by applying more shear load than allowable e.g 60000 N/m insted of 30740.79 N/m. See figure below.

Similarly we can get results for other shafts results are discussed later.



**User Defined / Allowable Load**

Nx   (N/m)

Ny   (N/m)

Nxy   (N/m)

Mx   (N)

My   (N)

Mxy   (N)

MOS

**Failure Theory**

Max Strain  
 Max Stress  
 Von Mises / Hoffman  
 Von Mises / Tsai-Hahn  
 Von Mises / Tsai-Hill  
**Von Mises / Modified Tsai-Wu**

Figure 6.4: Hypersizer window for allowable load

Failure Analysis		Strain Plot		Stress Plot		MOS Plot	Failure Envelope
Ply	MOS	Temp	Type	Limiting Failure Analysis	Location		
<input type="checkbox"/> 4	1.573	22.22 °C	Orthotropic	Tsai-Wu	Top		
<input type="checkbox"/> 4	1.836	22.22 °C	Orthotropic	Tsai-Wu	Middle		
<input type="checkbox"/> 4	1.775	22.22 °C	Orthotropic	Tsai-Wu	Bottom		
<input type="checkbox"/> 3	0.706	22.22 °C	Orthotropic	Tsai-Wu	Top		
<input type="checkbox"/> 3	0.627	22.22 °C	Orthotropic	Tsai-Wu	Middle		
<input type="checkbox"/> 3	0.405	22.22 °C	Orthotropic	Tsai-Wu	Bottom		
<input type="checkbox"/> 2	-0.079	22.22 °C	Orthotropic	Tsai-Wu	Top		
<input type="checkbox"/> 2	-0.182	22.22 °C	Orthotropic	Tsai-Wu	Middle		
<input type="checkbox"/> 2	-0.287	22.22 °C	Orthotropic	Tsai-Wu	Bottom		
<input type="checkbox"/> 1	-0.323	22.22 °C	Orthotropic	Tsai-Wu	Top		
<input type="checkbox"/> 1	-0.413	22.22 °C	Orthotropic	Tsai-Wu	Middle		
<input checked="" type="checkbox"/> 1	-0.488	22.22 °C	Orthotropic	Tsai-Wu	Bottom (Laminate Bottom)		

Figure 6.5: Ply failure window of Hypersizer

### 6.3.2 Ansys results

XY shear stress for applied torque of 1864 Nm is generated here. Boundary conditions are shaft is taken as fixed at one side and torque applied to other surface nodes. Nodal and Element both solution are shown here.

Ansys results for 72mm Filament wound shaft.

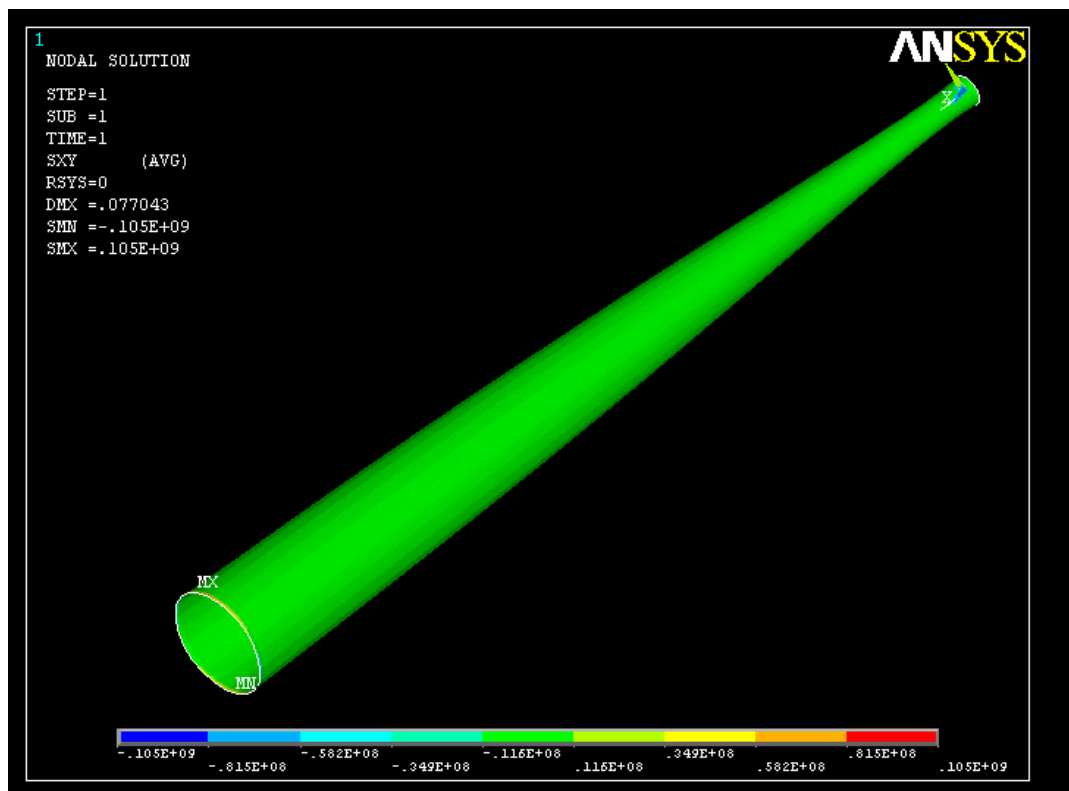


Figure 6.6: XY shear stress - Nodal solution for 72mm shaft

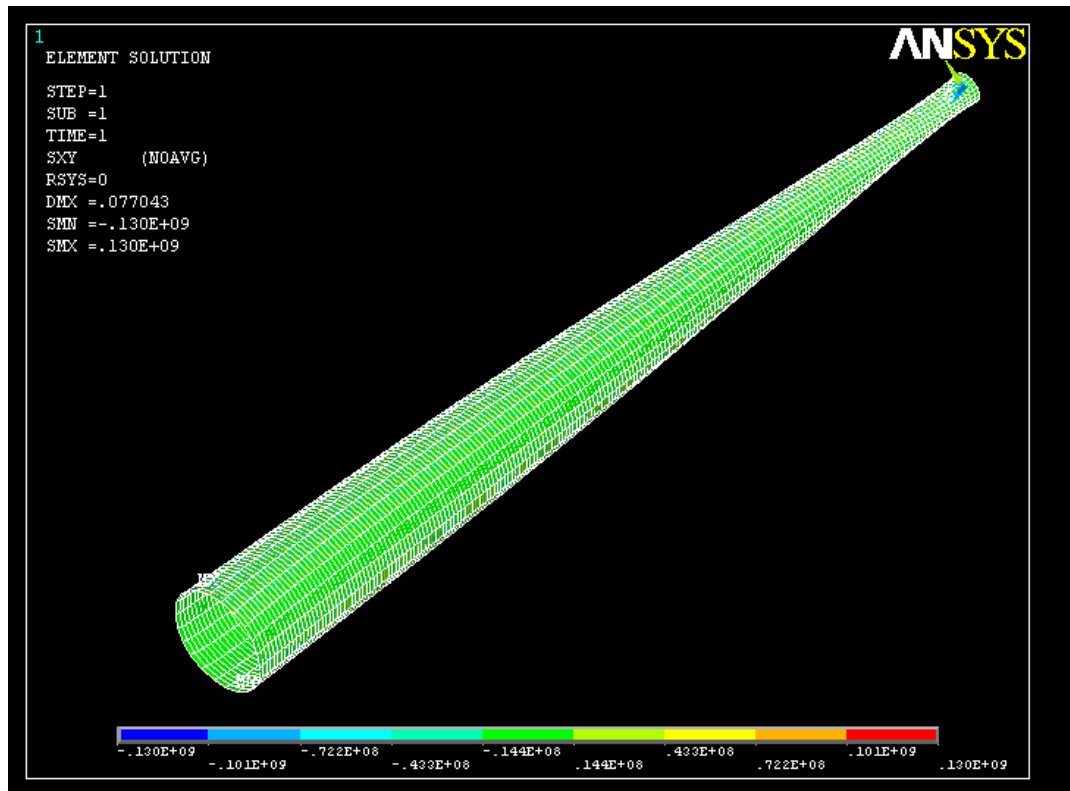


Figure 6.7: XY shear stress - Element solution for 72mm shaft

Also first lateral natural frequency is found using modal analysis and first mode is obtained by considering pinned-pinned boundary condition which is shown behind.

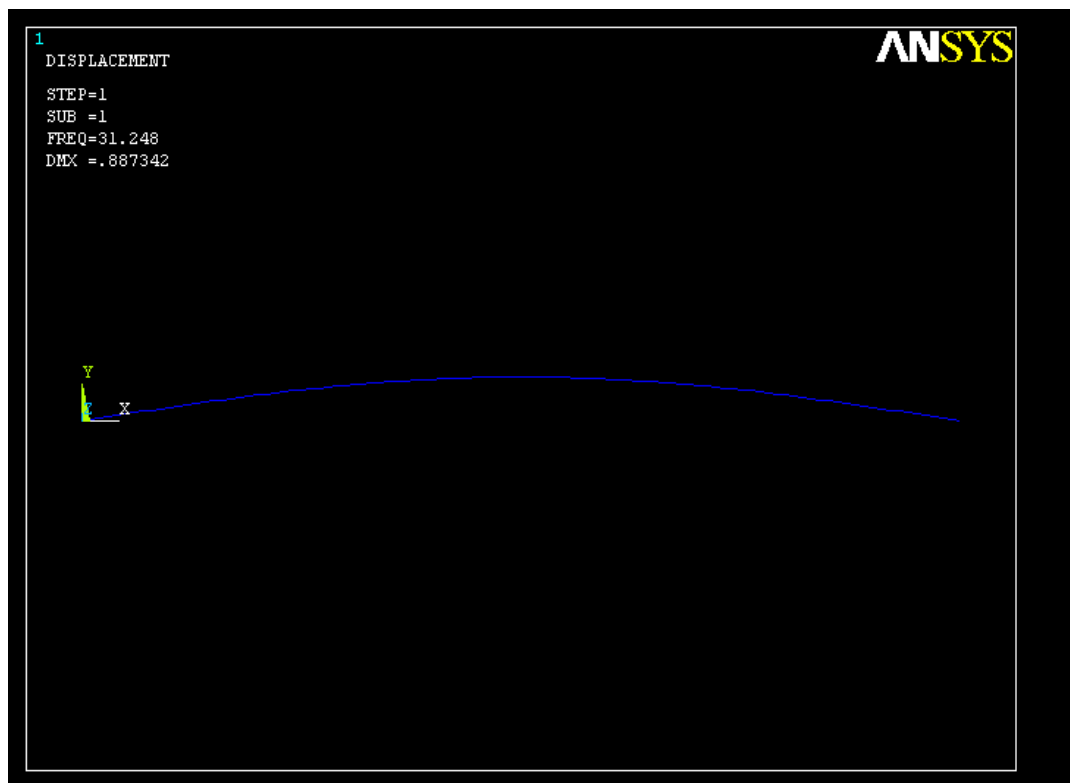


Figure 6.8: First mode of lateral natural frequency for 72mm shaft

Ansysis result for 50mm pull wound shaft.

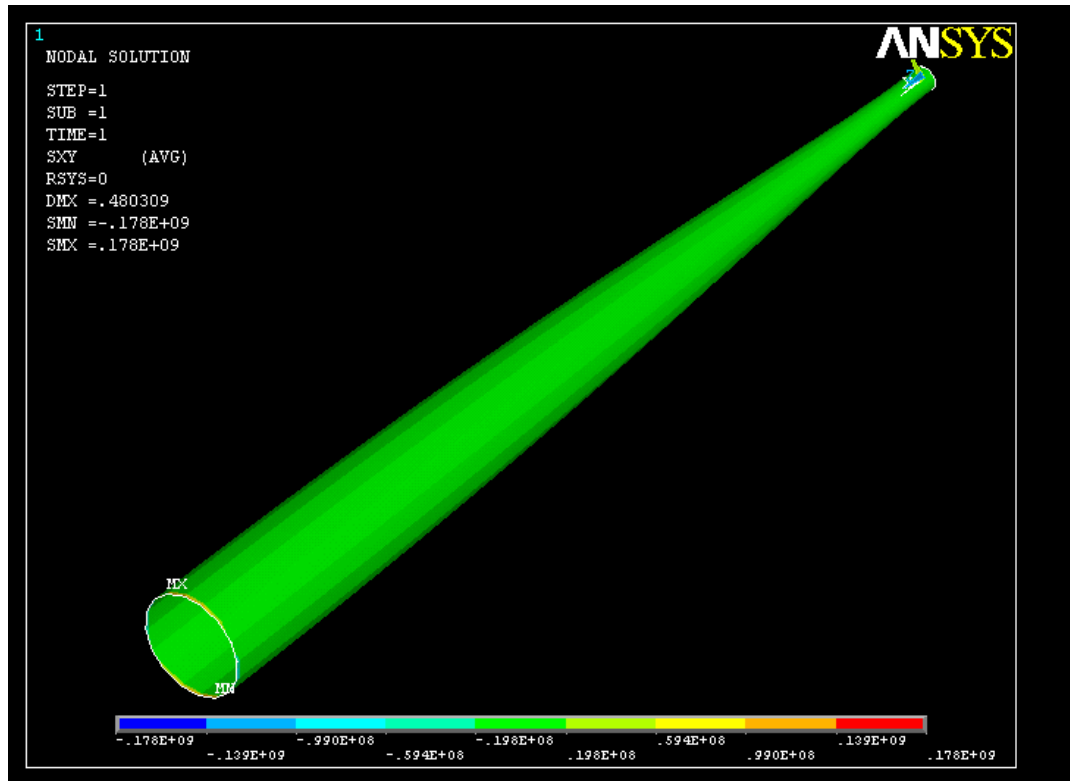


Figure 6.9: XY shear stress - Nodal solution for 50mm shaft

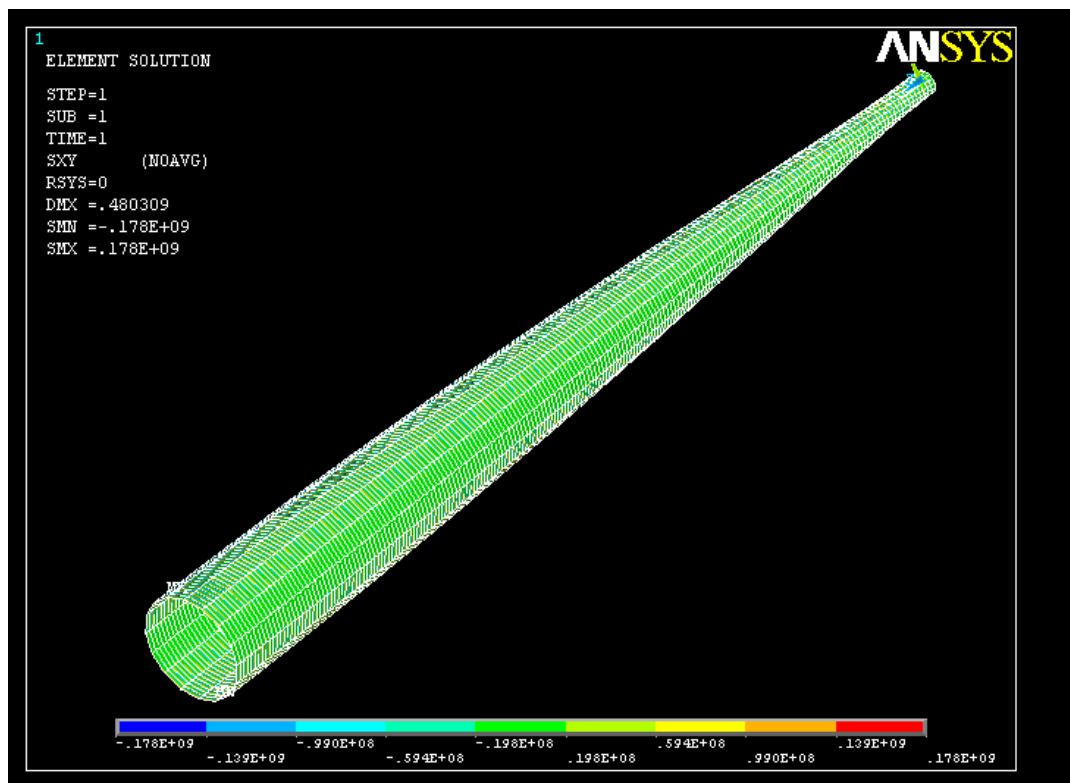


Figure 6.10: XY shear stress - Element solution for 50mm shaft

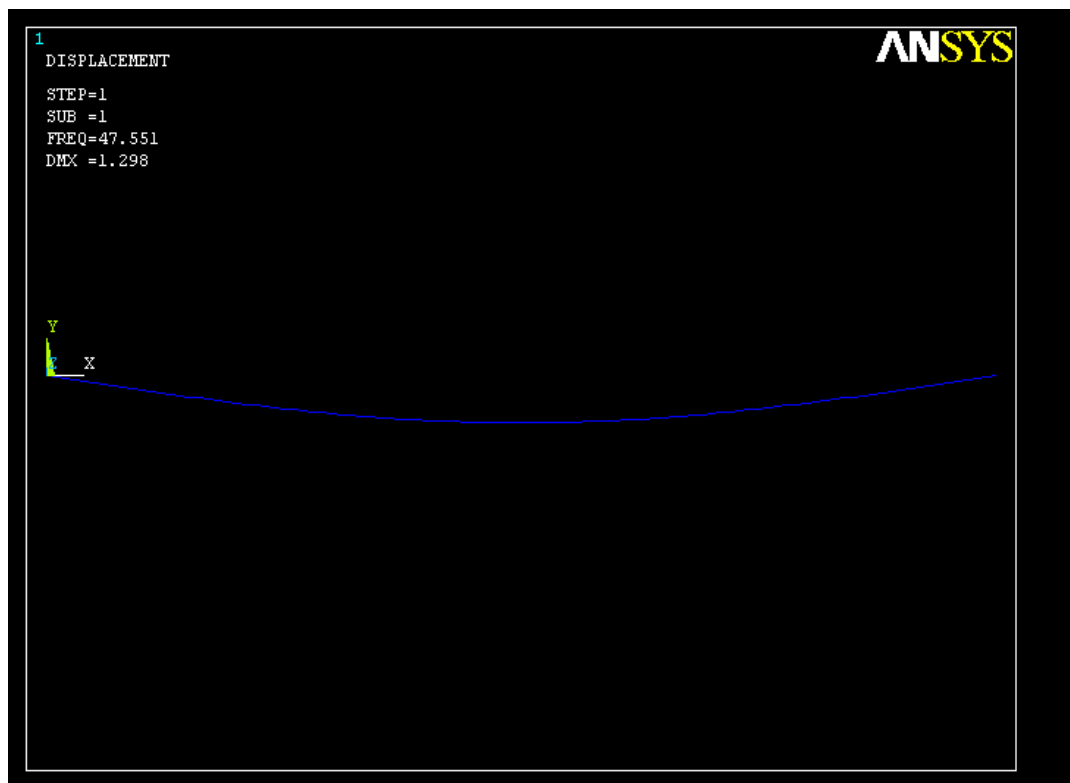


Figure 6.11: First mode of lateral natural frequency for 50mm shaft

## Ansysis result for 60.33mm shaft

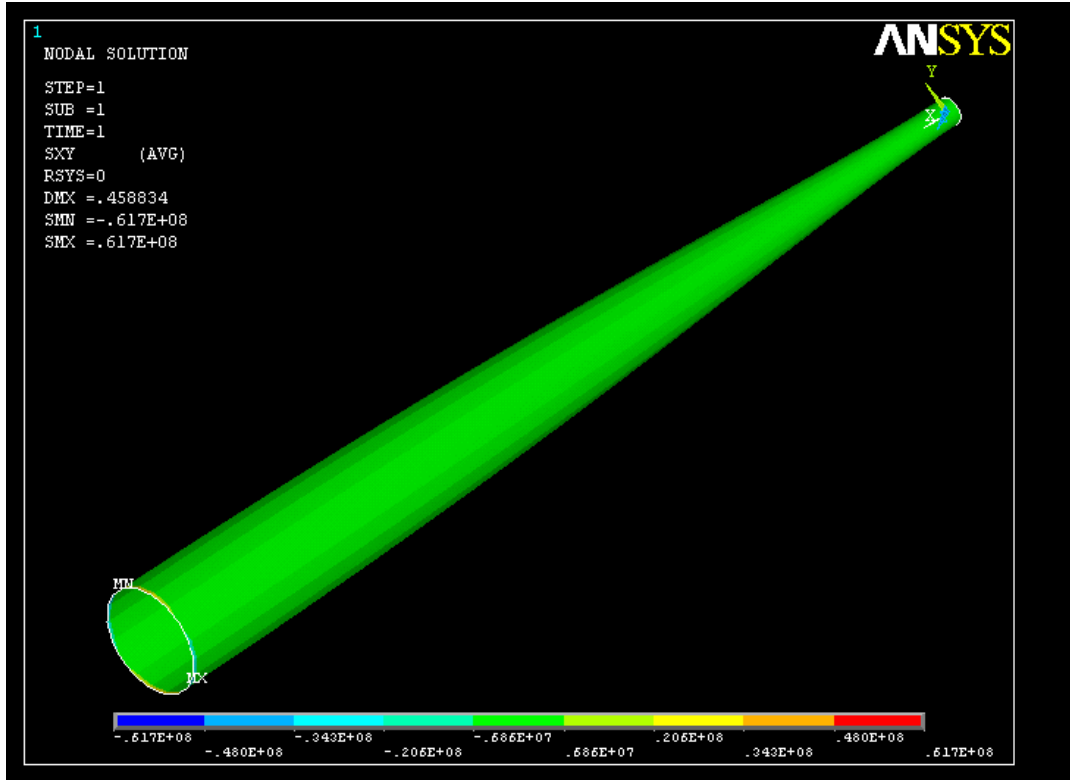


Figure 6.12: XY shear stress - Nodal solution for 60.33mm shaft



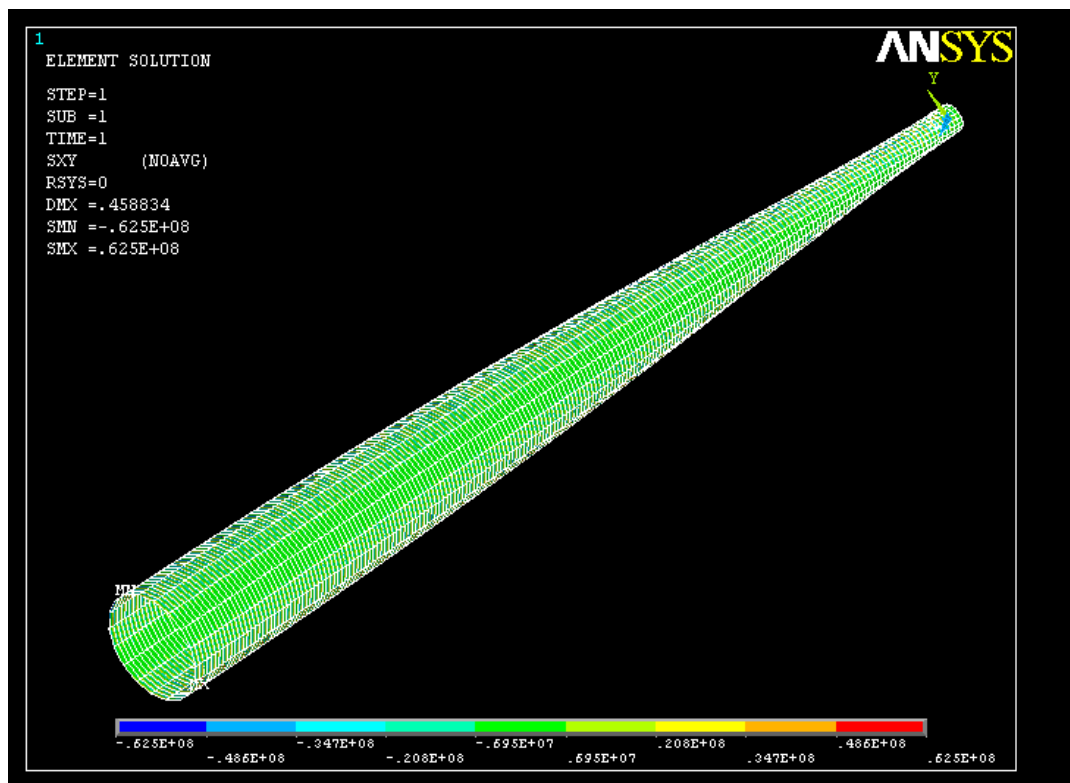


Figure 6.13: XY shear stress - Element solution for 60.33mm shaft

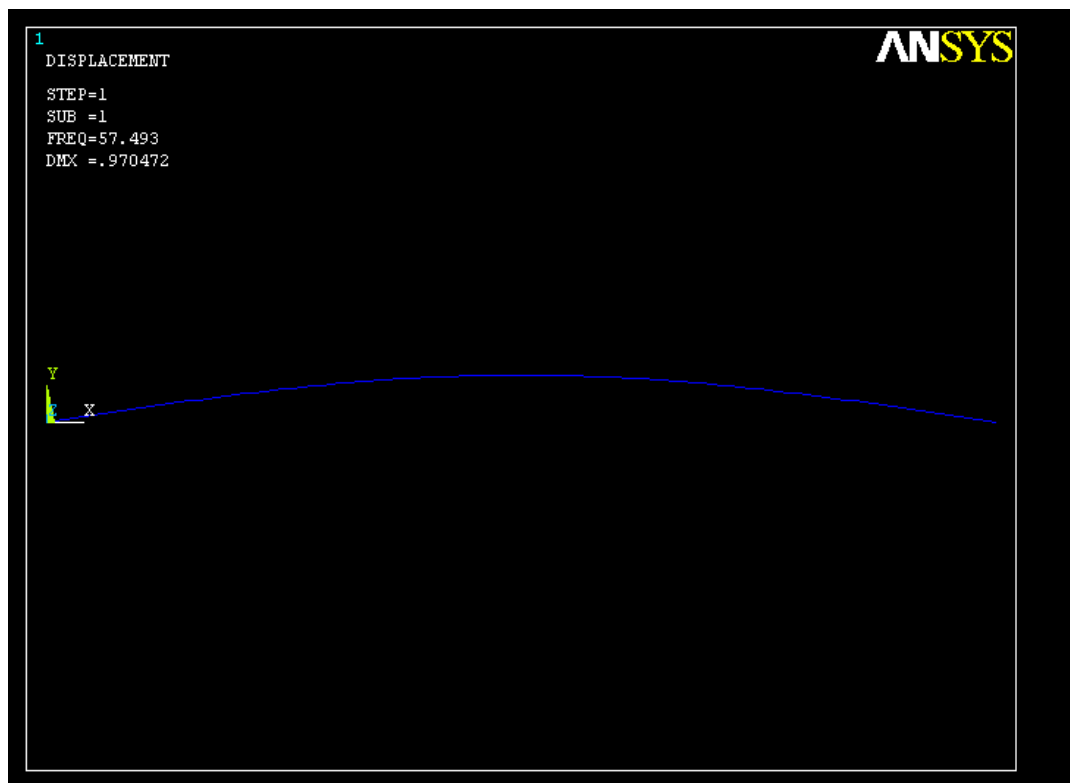


Figure 6.14: First mode of lateral natural frequency for 60.33mm shaft

### 6.3.3 Comparison

Comparison for 60.33 mm shaft is shown here. Here Theoretical, Hypersizer and practical results are shown.

Table 6.1: Comparison of theoretical, Hypersizer and practical result

Parameters	Theory	Hypersizer	Practical
Axial modulus	78.10 GPa	78.10 GPa	-
Axial strength	756.1 MPa	742.4 MPa	672 MPa
Shear strength	32.32 Mpa	31.39 MPa	-
Density	1443.38 $Kg/m^3$	-	-

Comparison of 60.33 mm shaft for maximum XY shear is shown by following figures.

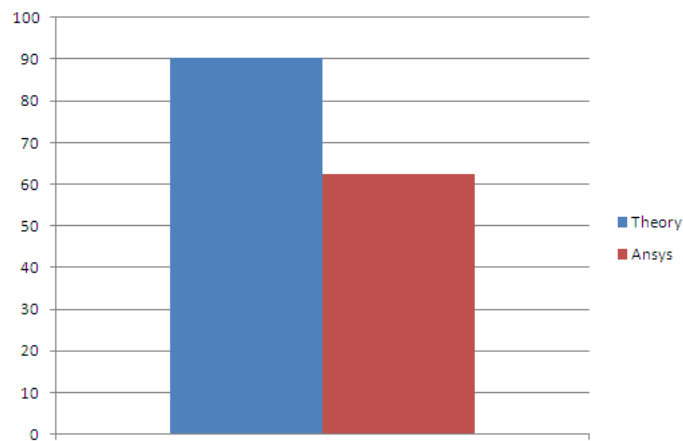


Figure 6.15: XY shear for 60.33mm shaft

Also comparison of analytical shear stress and frequency with shear stress and frequency found from FEA with Ansys are shown in following figures. Here 1, 2 and 3 indicates 72mm, 50mm and 60.33mm shafts respectively.

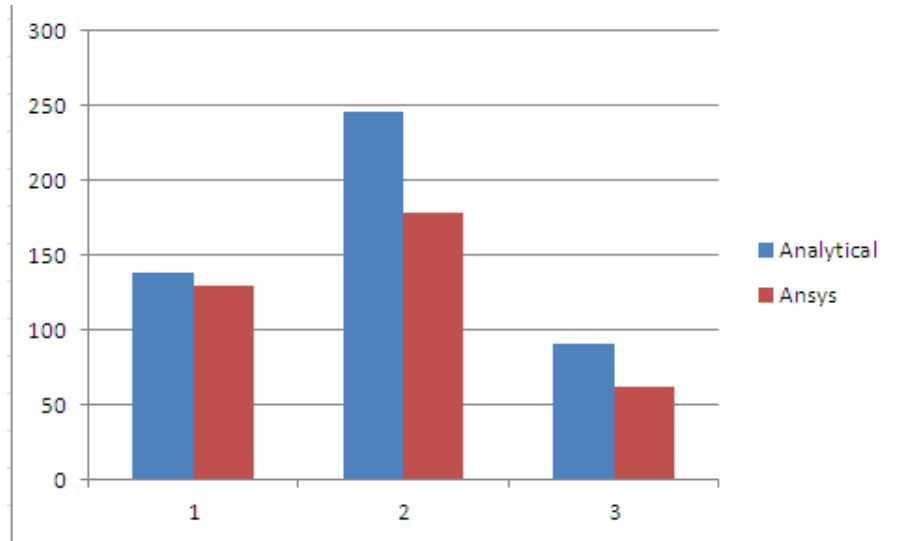


Figure 6.16: XY shear comparison - analytical and ansys

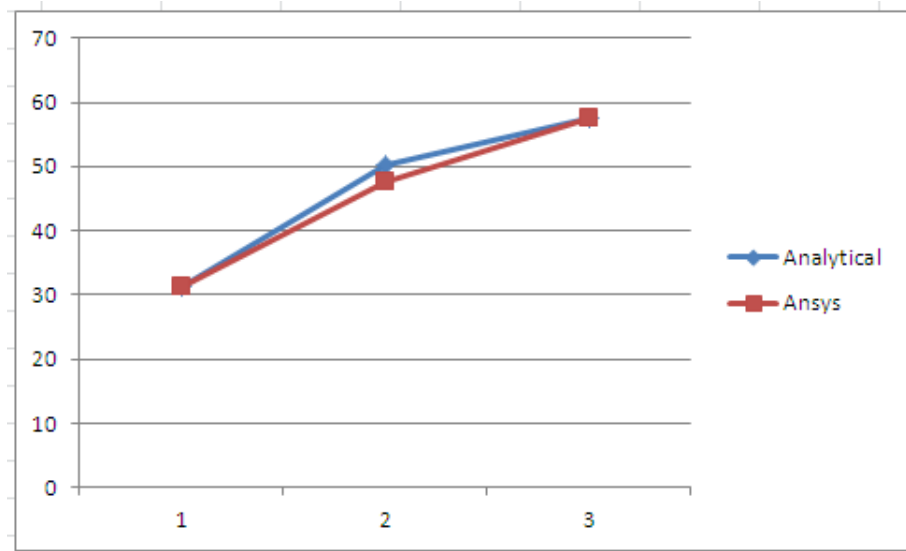


Figure 6.17: Lateral natural frequency comparison - analytical and ansys

# Chapter 7

## Optimum Design

### 7.1 New Layup arrangement

Previous study shows all shaft designs are not safe in torsion so  $\pm 45$  degree rovings should be added. Standard mats available in industries and their GSM are shown in following figure. For safety purpose design based on more fiber volume fraction should be selected. Therefore 60% fiber volume fraction are selected. If we inserts two  $\pm 45$  degree mats than thickness obtained by each mat according to equation of thickness is 0.572mm. Than to make bending matrix as zero, all layers are decided as below .

Table 7.1: Layer configuration for optimum shaft

Layer No.	Angle	Thickness in mm	No. of rovings
1	0	1.144	153
2	90	0.3665	1
3	45	0.286	mat
4	-45	0.286	mat
5	-45	0.286	mat
6	45	0.286	mat
7	90	0.3665	1
8	0	1.144	132

Items	Fibre type	0° gr/m <sup>2</sup>	+45° gr/m <sup>2</sup>	90° gr/m <sup>2</sup>	-45° gr/m <sup>2</sup>	CSM gr/m <sup>2</sup>	Stitch bonding gr/m <sup>2</sup>	Total Weight gr/m <sup>2</sup>
<i>* Ultralightweight carbon fabrics made of a new special technology ( ref. CARBON FABRICS )</i>								
CBX150*	CARBON	-	75	-	75	-	5	155
CBX200*	CARBON	-	100	-	100	-	5	205
CBX250*	CARBON	-	125	-	125	-	5	255
CBX300*	CARBON	-	150	-	150	-	5	305
CBX400*	CARBON	-	200	-	200	-	5	405
CBX450*	CARBON	-	225	-	225	-	5	455
CBX600*	CARBON	-	300	-	300	-	4	604
CBXS200*	CARBON	100	-	100	-	-	6	206
CBXS400*	CARBON	200	-	200	-	-	6	406
CBXS600*	CARBON	300	-	300	-	-	6	606

Figure 7.1: Standard Carbon fiber mats

## 7.2 Comparison between theoretical results and hypersizer results

Now all lamina properties are calculated from Halpin-Tsai equations[] and are as under

Table 7.2: Predication of different Lamina properties for JAITEC/Vinylester shaft

Parameter	Values
$E_1$	109.4 GPa
$E_2$	8 GPa
$G_{12}$	3.624 GPa
$\nu_{12}$	0.248
$\rho_c$	1536 Kg/m <sup>3</sup>
$(\sigma_1^T)_{ult}$	1398 MPa

On the basis of this properties theoretical and hypersizer solvers results are compared. Hypersizer result windows shows properties and failure envelopes.

Table 7.3: Predication of different Laminate properties for JAITEC/Vinylester shaft

Parameter	Values
$E_x$	68.80GPa
$E_y$	32.03 GPa
$G_{xy}$	10.45 GPa
$\nu_{xy}$	0.266
$\nu_{yx}$	0.124
$\sigma_{tL}$	477.3 MPa
$\tau_{xy}$	98.82 MPa

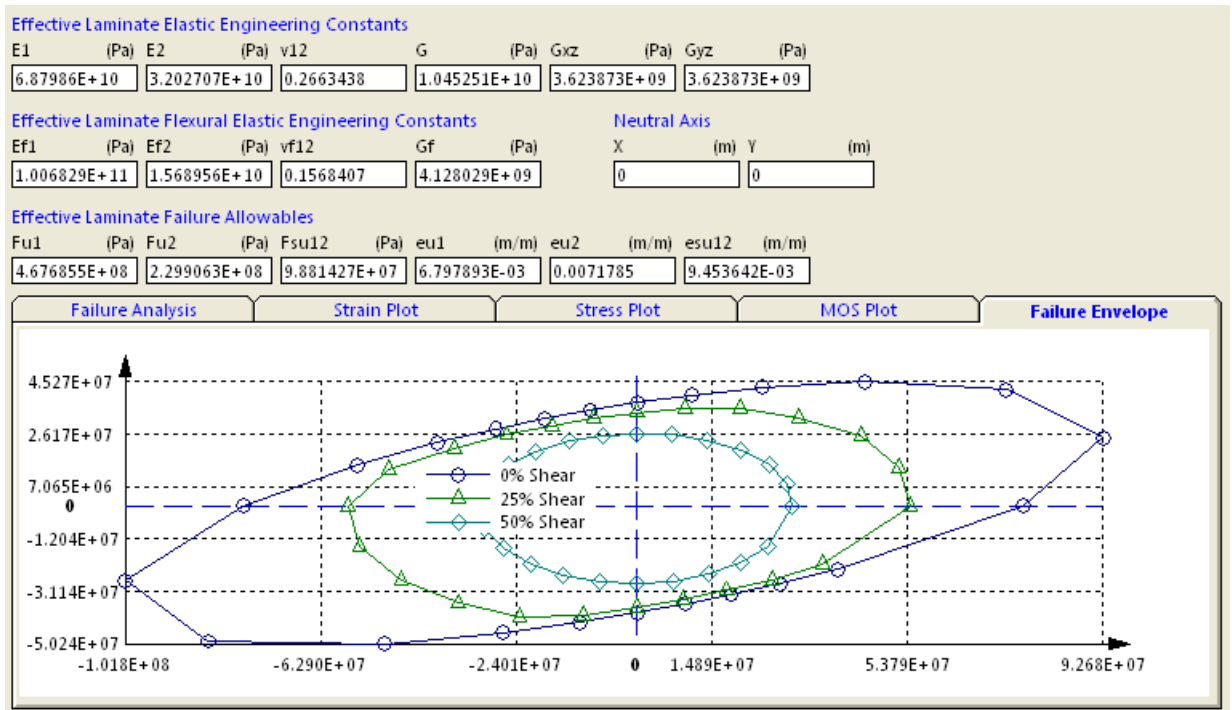


Figure 7.2: Hypersizer predicted properties for optimum design

## 7.3 Finite Element analysis

Following figures shows Nodal and element solution for XY shear using ANSYS shell99 element. Also first natural frequency and its mode shape is shown here.

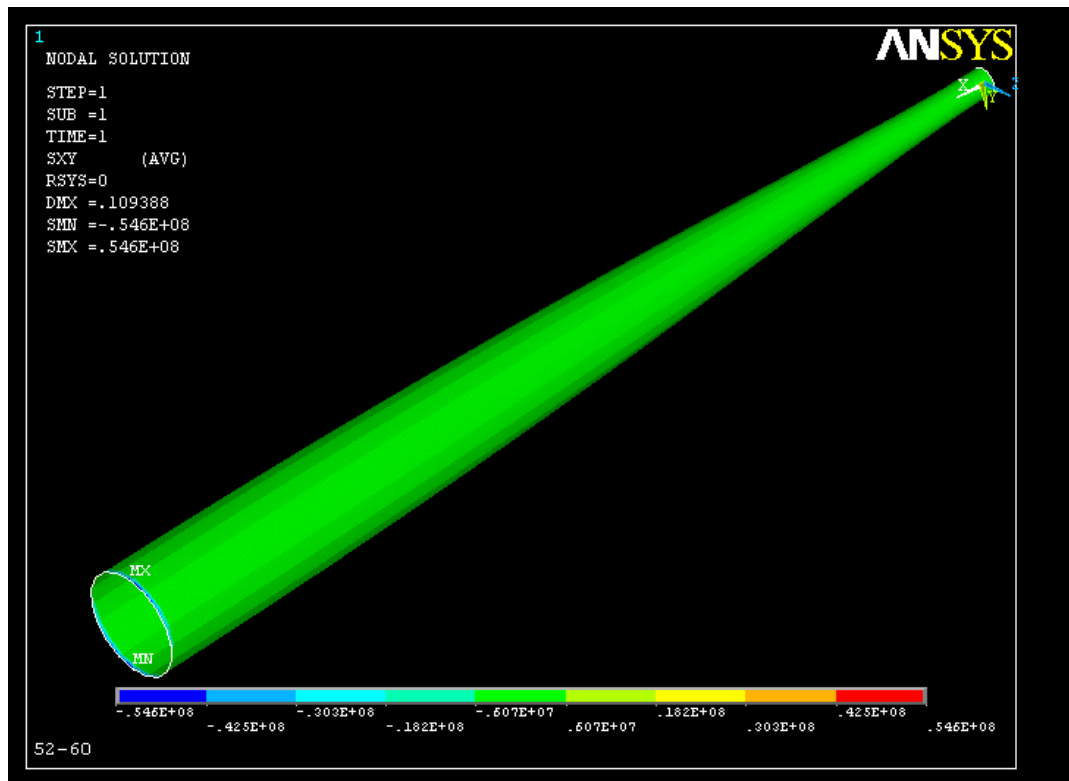


Figure 7.3: XY shear nodal solution



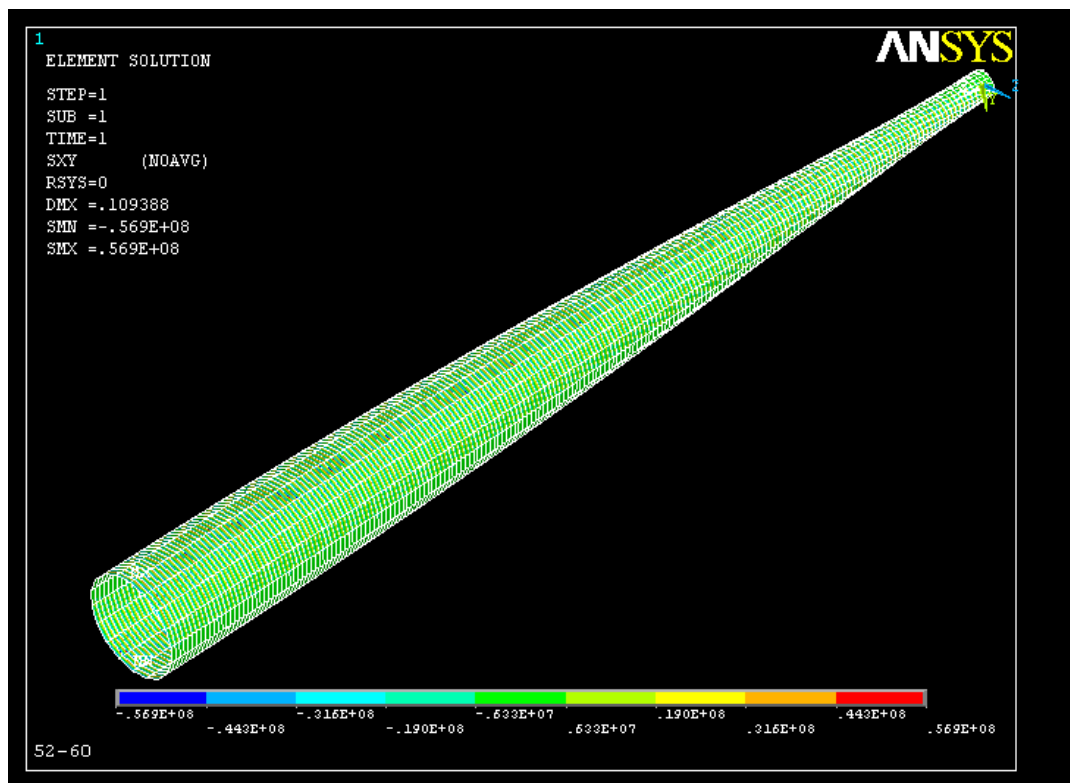


Figure 7.4: XY shear element solution

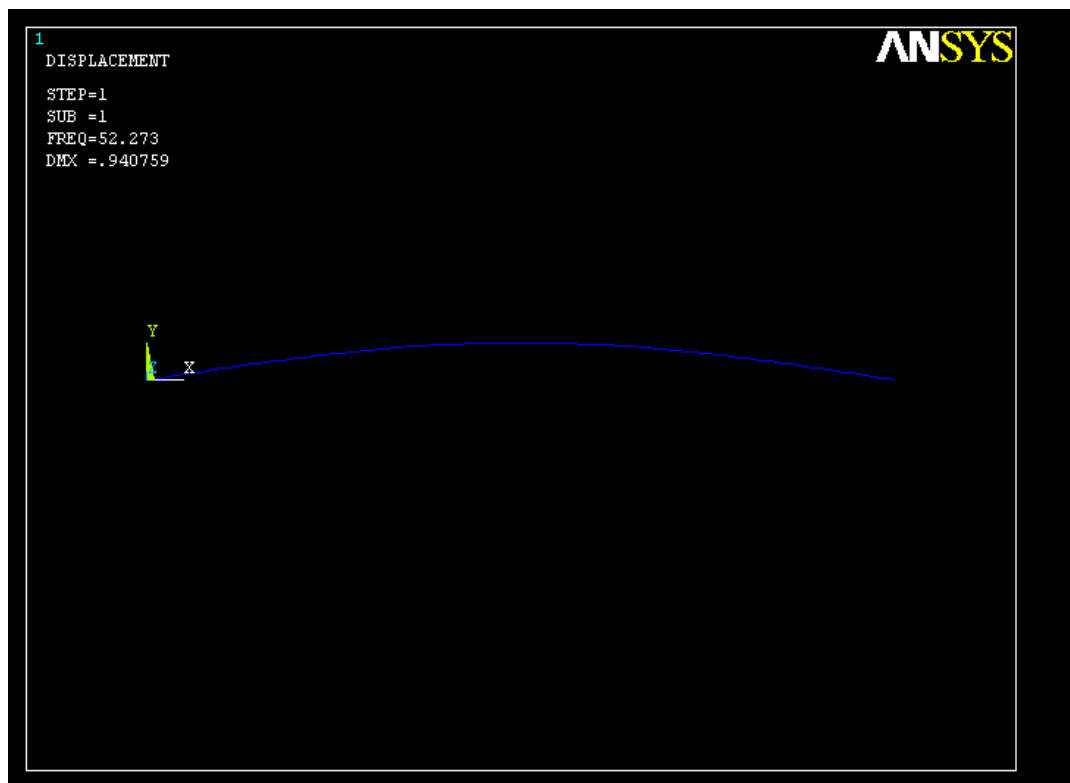


Figure 7.5: Modal analysis

## 7.4 Results and discussion

Theoretical Calculations and above analysis can be used to predict design safety. Hypersizer can be helpful to predict shear load that is responsible to predict ply failure. The maximum load that the laminate can withstand is 411560.6 N/m from this torque transmitting capacity 2039.32 Nm

Theoretically shear stress induced for 1864 torque transmission is 96.48 MPa. Calculation shows allowable shear stress is 98.82 MPa so torque transmitting capacity is 1909.09 Nm. Also ansys results are showing XY shear stress induced 56.9 MPa which is less than allowable stress. So design is safe in torque transmission

Now lateral natural frequency found from Euler-Bernouli equation is 52.35 Hz which is less than allowable frequency 46 Hz also ansys results are showing frequency = 52.25 Hz. Thus our design is safe on the basis of first lateral natural frequency.

Also torsional buckling capacity for this kind of shaft should be found. From equation this is obtained as 12430.23 Nm which is higher than torque transmission capacity so shaft will not buckle torsionally.

All design constraints are satisfied here so our design is safe.

# Chapter 8

## Design of adhesive joints in composite drive shafts

### 8.1 Adhesive joints

The joints used for connecting composite materials can be metallic or non-metallic. Steel fasteners, due to the possibility of galvanic corrosion with carbon-epoxy materials, are mainly made of titanium or stainless steel. Other alloys such as aluminum or steel can be used provided that no contact with the surface will occur.

Joints were divided into metal screws and rivets. Non-metallic connectors were created from reinforced thermoset or thermoplastic resins. By using this connection, structural weight reduces and corrosion problems disappear [12]. In this part, the thickness of the adhesive and the length of the adhesive bond were computed.

### 8.2 Calculation for length and thickness of joint

Our case is similar to case of shear stress in simple collar in which adhesive specifications can be described by following figure.

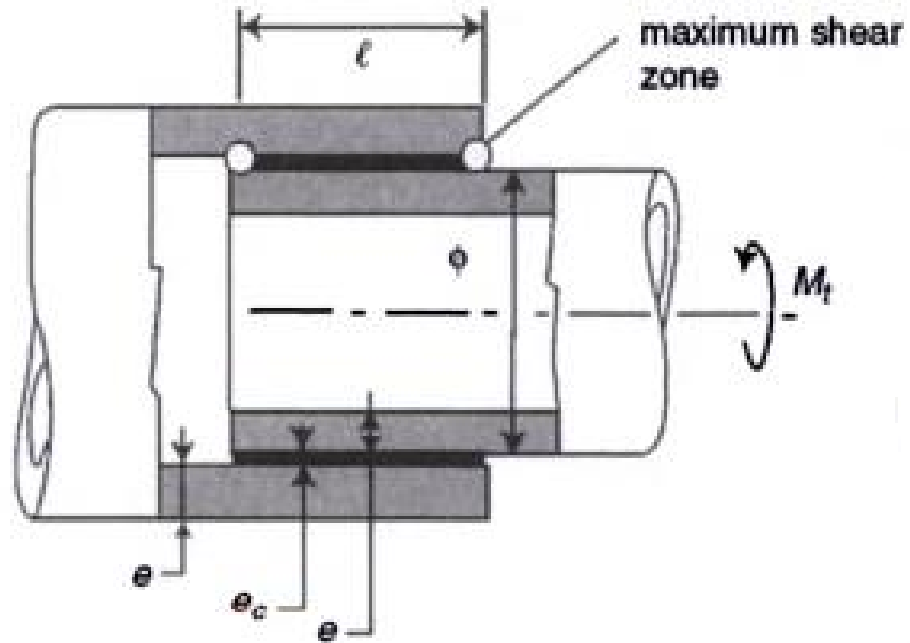


Figure 8.1: shear stress in cylindrical sleeve

According to Gay and Tsai the following correlations were used to calculate the required parameters [1]:

$$\tau_{avg} = \frac{2T}{\pi d_o^2 l} \leq 0.2 \times \tau_{adh}$$

$$\tau_{max} = \frac{a\tau_m}{\tanh a}$$

Where

$$a = \sqrt{\frac{G_c l^2}{2G e e_c}}$$

Now

$$\tau_{avg} = 7.24MPa$$

Here we are using epoxy adhesive which properties are described in Table. Following graph shows  $\tau_{max}$  vs  $\sqrt{e_c}$  results. Here adhesive length of 45mm is taken. By plotting the graph range we can find minimum adhesive thickness of 7.997 mm is required.

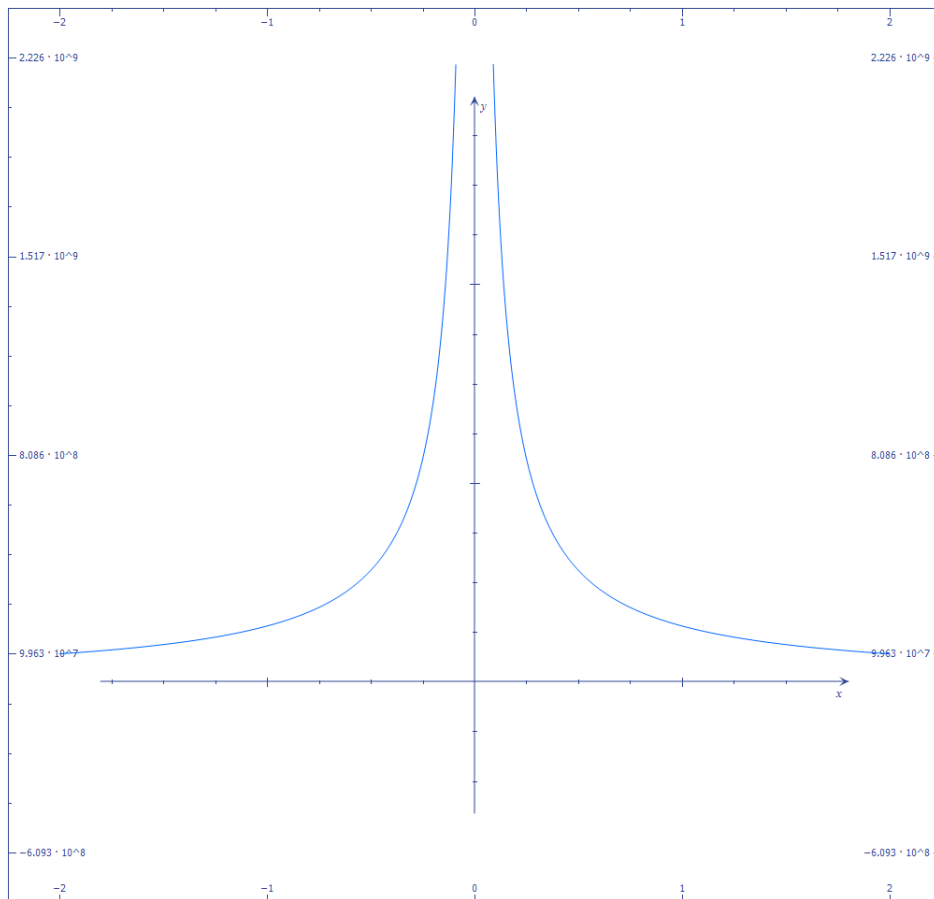


Figure 8.2:  $\tau_{max}$  vs  $\sqrt{e_c}$  graph for adhesive epoxy

# Chapter 9

## Conclusion and Future work

### 9.1 Concluding Remarks

- Here procedure to design a carbon fiber shaft is suggested which is useful to design any composite drive shaft. Drive shaft made up of Carbon/Epoxy and JAITEC/Vinylester multilayered composites has been designed.
- Research shows Micromechanics approach of Halpin-Tsai semi-empirical model is very useful and reliable for predictions of Lamina properties and from this predictions we can find Laminate properties for given fiber orientations.
- Research shows fiber orientation angle is very important parameter for design of shaft. Shaft's axial, transverse and shear strength and modulus are affected by different fiber angles. Also we can say that axial modulus which strongly affects Lateral natural frequency can be increased by increasing  $0^0$  rovings, shear strength can be increased by increasing  $45^0$  rovings and torsional buckling capacity can be increased by increasing  $90^0$  rovings. Here optimum fiber orientations are selected for given peak torque and design is analyzed for given constraints.
- Result of Finite Element Analysis by Ansys as considering shell element shows relatively near by values of stress and modes of vibrations which was obtained analytically. Also Hypersizer can be used to analyse design analytically.

## 9.2 Future scope

The shaft design discussed in this research shows only static performance of shaft but fatigue analysis of shaft is also one of the important topic for analysis in future.

When flanges are connected with shaft some other parameters can be considered in design like stress concentration and fracture mechanics which can be interesting topic for research.

Also optimum design for minimum cost or thickness can be developed by using different optimization techniques. We can also design a shaft based on an optimum fiber orientations for given properties with several optimization techniques. Optimization of design by Hypersizer software with coupling of FEA solvers like Msc-Nastran is interesting topic for industrial research.



# References

- [1] Rexnord addax. *Rexnord addax composite coupling catalog*. Rexnord Industries LLC, Fletcher Avenue, Lincoln, USA, 2007.
- [2] S. W. Tsai. D. Gay, S. V. Hoa. *Composite materials: design and application*. CRC press, 2004.
- [3] Isaac M. Daniel and Ori Ishair. *Engineering Mechanics of Composite Materials, Second Edition*. Oxford University Press, New-Delhi, India, 2005.
- [4] Fadi El-Chiti. *Experimental variability of E-Glass reinforced vinyl ester composites Fabricated by VARTM/SCRIMP*. Master degree thesis, The University of Maine, 2005.
- [5] Trinankur Hazra. *A low cost 2-axis plc controlled filament winding machine with simplified fiber winding angle and tension control system*. Thesis, Dalhousie University Halifax, Nova Scotia, March 2011.
- [6] John C. Hensley. *Cooling Tower Fundamentals, Second edition*. SPX cooling technology, USA, 2011.
- [7] K. C. Liu J. M. Corum, R. L. Battiste and M. B. Ruggles. *Basic Properties of Reference Crossply Carbon fiber composites*”, Oak ridge national laboratory. lockkekd martin, Department of Energy, US, 1996.
- [8] Autar K. Kaw. *Mechanics of Composite Material*. Taylor and Francis Group, London, New-York, 2006.
- [9] Hyonny Kim and Keith T. Kedward. *Stress Analysis of Adhesive Bonded Joints Under In-Plane Shear Loading*. University of California, Santa Barbara, 2007.
- [10] P. Mertiny and F. Ellyini. *Influence of the filament winding tension on physical and mechanical properties of reinforced composites*. Elsevier science ltd, London New-York, 2002.
- [11] Department of defense. *Composite materials handbook polymer matrix composites materials properties, Vol-3*. Department of Defense, USA, 2002.
- [12] Department of defense. *Composite materials handbook polymer matrix composites materials usage, design, and analysis, Vol-2*. Department of Defense, USA, 2002.
- [13] Shahzad Rahman and David A. Pecknold. *Micromechanics-based analysis of fiber- reinforced laminated composites*. Department of civil engineering University of Illinois Urbana, Illinois, september 1992.

- [14] Prof. M.V.Kavade Sagar D. Patil, Prof. D.S.Chavan. *Investigation of Composite Torsion Shaft for Torsional Buckling Analysis using Finite Element Analysis*. Rajarambapu Institute of Tecnology, Sakharale, 2012.
- [15] Gummadi Sanjay and Akula Jagadeesh Kumar. *Optimum Design and analysis of a composite drive shaft for an Automobile*. Master degree Thesis, Dept. of Mech. Engineering, Blekinge Institute of Technology, Swedon, 2007.
- [16] S. P. Timoshenko and J. N. Goodier. *Theory of Elasticity, Third Edition*. McGrow-Hill International Editions, Tokyo, 2002.
- [17] R.A. Chandrashekar T.K. Venkatesh T.Rangaswamy, S. Vijayarangan and K.Anantharaman. *Optimal design and analysis of automotive composit edrive shaft*. Dept. of Mech. Engineering, PSG College of Technology, Coimbatore, India, 2004.
- [18] Valery V. Vasiliev and Evgeny Morozov. *Mechanics and Analysis of Composite Materials*. Elsevier Science ltd, London, New-york, 2001.
- [19] Stephen W.Tsai. *Mechanics of Composite Materials, Part-2 Theoretical aspects*. Air force materials laboratory research, Ohio, 1966-1997.
- [20] A. Zureick and A. T. Nettles. *Composite Materials: Testing, Design, and Acceptance Criteria*. ASTM International, West Conshohocken, USA, 2002.